UNIVERSITÀ DEGLI STUDI DI PADOVA

Scuola di Ingegneria

Dipartimento di Ingegneria Civile, Edile ed Ambientale

Tesi di Laurea

MODELING CHLORIDE CIRCULATION AT PLYNLIMON CATCHMENTS, WALES

Relatore: Dott. Ing. Gianluca BOTTER

Correlatore: Dott. Paolo BENETTIN

Laureando: Carlo COMIN

Anno Accademico 2013-2014

Contents

List of Figures

List of Tables

Chapter 1

Introduction

Traditional hydrological modeling of catchments is based on rainfall-runoff models that aim to convert inputs into outputs within a defined control volume, oversimplifying in some cases all the processes taking place along this transformation. This choice is justified by the good performances that can be achieved in terms of water volumes, and is further supported by the evidence that the heterogeneity of subsurface environments prevents from having a satisfactory descripition of how water moves, mixes and finally reaches the basin closure section after its entrance as rainfall. Within this framework, however, several recent experimental and theoretical results have shown that event water constitutes only a part of stream water, that contains mainly *aged* particles, i.e. water particles injected at times preceding the event that directly caused the observed runoff, as illustrated in Figure 1.1. This evidence has often been addressed as *oldwaterparadox* and involves several important implications.

From the point of view of streamflows the distinction between the ages of water particles seems to be just a sophistication, since the aim is to estimate the amount of outflowing volumes, but it becomes essential when describing solute transport within a catchment, since the chemical compositions of those outflowing volumes is strictly related to the time water particles have spent within the catchment. This remark is clear for reactive solutes that can undergo physical, chemical and biological time-driven transformations in subsurface environments, but it is fundamental also in assessing the persistence of conservative solutes within defined environments and conditions, involving several environmental issues, which include the effects of atmospheric pollution on land water resources, the fate of injected compounds that can be toxic for plants, aquatic fauna and human health and the effects of land use management for agricultural and industrial purposes.

Recent studies have built a robust theoretical framework to describe the time spent by water particles within a catchment, based on a stochastic formulation of the transport problem. Supposing each rainfall event con-

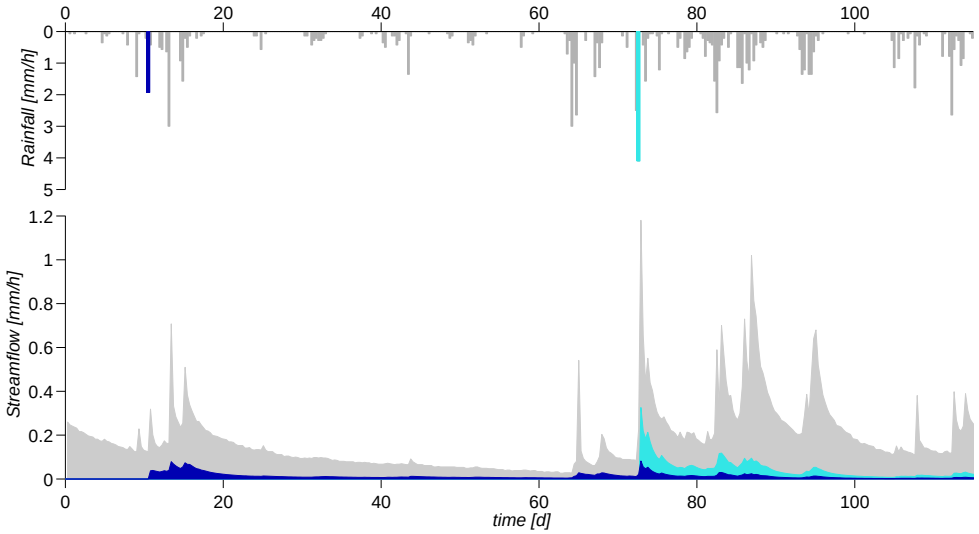

Figure 1.1: *Example illustrating the old water paradox: total discharge is mainly made up of 'aged' water*

stituted by a number of single water particles that enter the system (i.e. the catchment) at a fixed time, it is possible to describe their fate by using random variables and their probability density functions, thereby providing a stochastic description of how the catchment retain and release water. The travel time, defined as the time elapsed from the injection of a particle into the system and the exit through any of its boundaries, is the major descriptor of the flow and transport dynamics taking place in heterogeneous hydrologic systems. Recently analytical expressions for travel time distributions have been obtained as a function of hydrological features of the catchment, that are clearly time-dependent, implying the time dependency of travel time distributions; the non-stationary nature allows for an improved description of catchment dynamics, since this approach is able to detect the different responses basin gaves depending on its conditions.

The formulation of transport by travel time distributions is here applied to a small Welsh catchment. Besides data availability, the basin reveals interesting for the relatively high quantity of rainfall falling every year on this zone, in accordance to United Kingdom wet climate, and for the total absence of human activities within the area, allowing for a totally natural landscape. The theoretical framework is presented in Chapter 2, while the description of the area in Chapter 3; Chapters 4, 5 and 6 describe how the model is set and the obtained results, in terms of hydological fluxes, chloride transport modeling and travel time distributions. These results are briefly discussed in Chapter 7, and finally conclusions are reported in Chapter 8.

Chapter 2

Travel Time Distributions for Water and Solutes

2.1 Hydrological flows as functions of TTD's

The theoretical approach to TTDs starts from the definition of a control volume V which represents a hillslope, a catchment or a subcatchment of a river basin. Some hypoteses are made concerning V as matter of simplicity and to better focus on the main issue: lateral flux through volume boundaries is neglected, as well as deep losses and recharge terms bypassing the catchment control section. The only input to V is rainfall $J(t)$, which enters the system with a solute concentration $C_J(t)$. Total output flux is given by the sum of water fluxes leaving the control volume as evapotranspiration $ET(t)$ and streamflow $Q(t)$, each associated to an output solute flux: $\phi_{ET}(t)$ and $\phi_Q(t)$, respectively. The balance equations for water storage $S(t)$ and solute mass storage $M(t)$ within V are consequently expressed as:

$$\frac{dS(t)}{dt} = J(t) - Q(t) - ET(t) \tag{2.1}$$

$$\frac{dM(t)}{dt} = \phi_J(t) - \phi_Q(t) - \phi_{ET} + \left(\frac{dM}{dt}\right)_{react} \tag{2.2}$$

where $\phi_J(t)$ is the solute input through rainfall. Each solute flux ϕ_i (expressed as mass/time) is directly linked to the corresponding water flux by means of concentration C_i (e.g. $\phi_J(t) = J(t)C_J(t)$). The term $(dM/dt)_{react}$ defines all the mass variations caused by biological, chemical or physical transformations taking place within the system.

To describe the transport mechanisms within V, rainfall inputs are thought of as a number of water particles injected at a fixed time instant t_i. The time elapsed between the entrance of a particle within V and its exit through discharge or evapotranspiration at time t_{out} is called exit time

$T_{ex} = t_{out} - t_i$, and it is thought of as a random variable, whose probability density function (pdf) is p_{ex}. T_{ex} is strictly dependent on the injection time and on the whole series of states experienced by the system after the injection due to rainfall forcings, and thus, to stress these dependencies, the notation $p_{ex}(t|t_i; J)$ will be employed (i.e. $p_{ex}(t|t_i; J)$ represents the fraction of water particles injected in t_i, that exit the system in the interval $[t, t + dt]$). Accordingly, $P_{ex}(t - t_i|t_i; J)$ is the exceedance cumulative probability of particles injected in t_i (i.e. $P_{ex}(t - t_i|t_i; J)$ represents the fraction of water particles injected in t_i and still inside V at time t) [*Botter et al.*, 2010]. With the aim of determining the age of water particles leaving V, it is possible to express the water storage mass balance as a function of exit time distribution as:

$$S(t) = \int_{-\infty}^{t} J(t_i)\, P_{ex}(t - t_i|t_i; J)\, dt_i \tag{2.3}$$

Differentiating with respect to time, and using the Leibniz rule, one gets:

$$\frac{dS(t)}{dt} = J(t) - \int_{-\infty}^{t} J(t_i)\, p_{ex}(t - t_i|t_i; J)\, dt_i \tag{2.4}$$

Comparing equations (2.1) and (2.4) the following relation is obtained:

$$Q(t) + ET(t) = \int_{-\infty}^{t} J(t_i)\, p_{ex}(t - t_i|t_i; J)\, dt_i \tag{2.5}$$

which expresses the overall output fluxes ($Q(t)$ and $ET(t)$) as a function of input J and of the conditional exit time pdf.

In order to separate the overall output flux into its single terms $Q(t)$ and $ET(t)$, the following definitions are introduced: the travel time T_t is the time elapsed between the injection of the particle and its exit as discharge, and the evapotranspiration time T_{et} is the time elapsed between the injection and the release through the evapotranspiration flux. Hence, the exit time of a particle can be equal to its travel time, if the particle exits as Q, or to its evapotranspiration time, if the particle exits as ET. Both T_t and T_{et} are considered as random variables characterized, respectively, by the pdfs $p_t(t|t_i; J)$ and $p_{et}(t|t_i; J)$. The separation of output fluxes is controlled by the function $\theta(t_i)$, which expresses the probability that a water particle injected at t_i will leave the system through Q, that can be also seen as the fraction of water particles injected at t_i exiting V as Q; consequently, $(1 - \theta(t_i))$ will be the fraction of water particles injected at t_i exiting V as ET. According to these definitions it is possible to express the exit time pdf as:

$$p_{ex}(t|t_i; J) = \theta(t_i)\, p_t(t|t_i; J) + (1 - \theta(t_i))\; p_{et}(t|t_i; J) \tag{2.6}$$

Inserting equation (2.6) into (2.5) and separating the contributions due to discharge and evapotranspiration, the following relations are obtained:

$$Q(t) = \int_{-\infty}^{t} J(t_i)\,\theta(t_i)\,p_t(t-t_i|t_i;J)\,dt_i \tag{2.7}$$

$$ET(t) = \int_{-\infty}^{t} J(t_i)\;(1-\theta(t_i))\;p_{et}(t-t_i|t_i;J)\,dt_i \tag{2.8}$$

Equations (2.7) and (2.8) express the single ouput fluxes as function of input $J(t)$ through their respective transfer function, that is represented by the conditional travel or evapotranspiration time pdf.

2.2 Coupling water flows and solute transport

The scheme outlined above is now used to describe the transport of solutes through the system, from the injection into the control volume as rainfall, following water particles' fate to the exit via streamflow or evapotranspiration. A single value of concentration is considered for the whole storage, since it is assumed that the concentration is not affected by the position within V, hypotesis that is legitimate when nonpoint sources and heterogeneous hydrologic media are considered [*Botter et al.*, 2005,2009, *Rinaldo et al.*, 2006a,2006b].

According to the definitions given in the previous section, and in analogy with equation (2.3), it is possible to express the stored mass within V at time t as a function of exit time distribution as:

$$M(t) = \int_{-\infty}^{t} J(t_i)\,C(t-t_i,t_i)\,P_{ex}(t-t_i|J)\,dt_i \tag{2.9}$$

Equation (2.9) defines the stored $M(t)$ as the sum of mass entered into the system before t (represented by the mass flux $J(t_i)C(t-t_i,t_i)$) and not outflown yet (given by the exceedance cumulative probability $P_{ex}(t-t_i|J)$. The notation $C(t-t_i,t_i)$ stresses the dependence of concentration on injection time t_i and (for reactive solutes undergoing biological/chemical/physical reactions) on the time $t-t_i$, that is the time spent inside the control volume.

Deriving equation (2.9) with respect to t, one gets:

$$\begin{aligned}\frac{dM(t)}{dt} = &+ J(t)\,C_J(t)\\ &- \int_{-\infty}^{t} J(t_i)\,C(t-t_i,t_i)\,p_{ex}(t-t_i|t_i;J)\,dt_i\\ &+ \int_{-\infty}^{t} J(t_i)\,P_{ex}(t-t_i|t_i;J)\,\frac{dC(t-t_i,t_i)}{dt}\,dt_i\end{aligned} \tag{2.10}$$

The solute concentration C can be assumed to change in time only due to the reactions involving reactive solutes, leading to the term $(\frac{dM}{dt})_{react}$ in equation (2.2) to be expressed as:

$$\left(\frac{dM}{dt}\right)_{react} = \int_{-\infty}^{t} J(t_i)\, P_{ex}(t - t_i|t_i; J)\, \frac{dC(t - t_i, t_i)}{dt}\, dt_i \tag{2.11}$$

that corresponds to the third term of the sum in right-hand side of equation (2.10). Consequently, inserting equation (2.11) into (2.2) and comparing with equation (2.10), the overall solute output flux at t is expressed as:

$$\phi_Q(t) + \phi_E(t) = \int_{-\infty}^{t} J(t_i)\, C(t - t_i, t_i)\, p_{ex}(t - t_i|t_i; J)\, dt_i \tag{2.12}$$

It is again possible to observe the analogy with equation (2.5), with the only additional term of concentration C. As already done, employing equation (2.6), the single contributions to output flux can be separated into those specifically associated with Q and ET:

$$\phi_Q(t) = \int_{-\infty}^{t} J(t_i)\, \theta(t_i)\, C(t - t_i, t_i)\, p_t(t - t_i|t_i; J)\, dt_i \tag{2.13}$$

$$\phi_{ET}(t) = \int_{-\infty}^{t} J(t_i)(1 - \theta(t_i))C(t - t_i, t_i)p_{et}(t - t_i|t_i; J)dt_i \tag{2.14}$$

2.3 The mixing scheme

Section 2.1 provided the expressions for discharge and evapotranspiration flows exiting the control volume V as function of Travel or Evapotranspiration times, respectively (equations (2.7) and (2.8)). To derive an analytical expression for the distributions as function of the involved hydrological quantities, it is necessary to introduce an assumption on how water is released from V, that means assuming a suitable scheme of how water mixes within V: in fact, it is possible that stream water is mainly composed by water that was already stored within the V, that was mobilized and pushed towards the outlet by the new incoming water; however it is possible that subsurface structure leads to the formation of preferential pathways, through which recently entered particles can fastly reach the channel, determining a priority for new water. Between these extremes infinite ways for new particles to mix with the old ones are possible, and among them here a simple, non parametric scheme is assumed: water particles that leave the system are randomly sampled among all the water particles contained in V, that means that at a fixed time they are released in the same proportion as they are present within the system at that time. This scheme will be addressed as random

sampling (RS) scheme and, physically, the situation can represent a heterogeneous system, in which the randomness of involved processes (infiltration, flow pathways, capillary raise, root distribution) is prevalent.

In mathematical terms RS scheme can be expressed as:

$$\frac{flow\ due\ to\ t_i}{total\ flow} = \frac{storage\ due\ to\ t_i}{total\ S(t)} \tag{2.15}$$

The l.h.s. of equation (2.15) expresses the contribution to the total flow of water particles injected in V at time t_i, while the r.h.s., instead, represents the relative contribution of the same particles to the total storage $S(t)$. These relations can be written for both Q and ET as:

$$\frac{J(t_i)\,\theta(t_i)\,p_t(t-t_i|t_i)}{Q(t)} = \frac{J(t_i)\,P_{ex}(t-t_i|t_i)}{S(t)} \tag{2.16}$$

$$\frac{J(t_i)\,[1-\theta(t_i)]\,p_{et}(t-t_i|t_i)}{ET(t)} = \frac{J(t_i)\,P_{ex}(t-t_i|t_i)}{S(t)} \tag{2.17}$$

2.4 TTDs conditional to injection time

The definition of a mixing scheme allows for an analytical expression of $p_t(t-t_i|t_i)$ and $p_{et}(t-t_i|t_i)$: in fact, isolating these terms from equations (2.16) and (2.17) one gets:

$$p_t(t-t_i|t_i) = \frac{Q(t)\,P_{ex}(t-t_i|t_i)}{\theta(t_i)\,S(t)} \tag{2.18}$$

$$p_{et}(t-t_i|t_i) = \frac{ET(t)\,P_{ex}(t-t_i|t_i)}{[1-\theta(t_i)]\,S(t)} \tag{2.19}$$

Differentiating equation (2.6) the following equation is obtained:

$$\frac{dP_{ex}(t|t_i)}{dt} = -\,\theta(t_i)\,p_t(t|t_i) - [1-\theta(t_i)]\,p_{et}(t|t_i) \tag{2.20}$$

and inserting equations (2.18) and (2.19) into (2.20):

$$\frac{dP_{ex}(t-t_i|t_i)}{dt} = -(Q(t)+ET(t))\,\frac{P_{ex}(t-t_i|t_i)}{S(t)} \tag{2.21}$$

Equation (2.21) is a differential equation in P_{ex} which can be exactly integrated between t_i and t by imposing the initial condition $P_{ex}(0|t_i)=1$,

leading to the following expression for the conditional exceedance probability of T_{ex}:

$$P_{ex}(t - t_i|t_i) \;=\; \exp\left(- \int_{t_i}^{t} \frac{Q(x) + ET(x)}{S(x)} dx \right) \tag{2.22}$$

The expressions for the pdfs, in the case of a random sampled storage, are obtained inserting equation (2.22) into (2.18) and (2.19):

$$p_t(t - t_i|t_i) = \frac{Q(t)}{S(t)\,\theta(t_i)} \exp\left(- \int_{t_i}^{t} \frac{Q(x) + ET(x)}{S(x)} dx \right) \tag{2.23}$$

$$p_{et}(t - t_i|t_i) = \frac{ET(t)}{S(t)\,(1 - \theta(t_i))} \exp\left(- \int_{t_i}^{t} \frac{Q(x) + ET(x)}{S(x)} dx \right) \tag{2.24}$$

The Travel and Evapotranspiration times pdf were finally expressed in terms of the fluxes and of the storage involved in the soil moisture balance, that can be derived by means of an hydrological model. The term $\theta(t_i)$ can in turn be expressed as a function of system hydrological quantities by imposing the normalization condition to the travel time pdf:

$$\int_0^{\infty} p_t(\tau|t_i)\, d\tau = 1 \tag{2.25}$$

and inserting equation (2.23) into equation (2.25), isolating $\theta(t_i)$, one gets:

$$\theta(t_i) = \int_{t_i}^{\infty} \frac{Q(\tau)}{S(\tau)} \exp\left[- \int_{t_i}^{\tau} \frac{Q(x) + ET(x)}{S(x)} dx \right] d\tau \tag{2.26}$$

Equation (2.26) clearly shows that the value of θ at a given time t_i, i.e. the probability that the particle will be released as streamflow, depends on the system states coming after the injection time t_i.

2.5 TTDs conditional to exit time

Sections 2.1 and 2.4 gave the definition of the travel time as a random variable and an analytical expression for its pdf was derived. The perspective was to follow the fate of a water particle injected at a fixed time, evaluating from a stochastic point of view the time it takes to exit from the control volume. It is possible however to keep another perspective in describing the travel time distributions: the general idea is to fix a sampling time at the outlet and to evaluate the age distribution of the sampled water particles in order to weight the contribution of past rainfall events to present discharge, i.e. to define a distribution conditional to the exit time, $p'_t(t - t_i|t)$. Generally

p_t and p'_t are different due to the unsteady state of the system [*Niemi*, 1977] (they coincide only in very special circumstances, see [*Rinaldo et al.*, 2011]) but related by Niemi's theorem:

$$J(t_i)\,\theta(t_i)\,p_t(t-t_i,t_i) = Q(t)\,p'_t(t-t_i,t) \tag{2.27}$$

Physically the l.h.s. of the relation represents the fraction of particles entered at t_i, that will leave the system as Q at the subsequent time t; instead, the r.h.s. represents the fraction of particles exiting as Q at time t, that entered at the past time t_i.

Isolating the term $p'_t(t-t_i|t)$ in equation (2.27) one gets:

$$p'_t(t-t_i,t) \;= \frac{\theta(t_i)}{Q(t)}\,J(t_i)\,p_t(t-t_i,t_i) \tag{2.28}$$

and inserting the expression of p_t given by equation (2.23) the expression for the TTD conditional to exit time is obtained:

$$p'_t(t-t_i|t) = \frac{J(t_i)}{S(t)}\exp\left(-\int_{t_i}^{t}\frac{Q(x)+ET(x)}{S(x)}dx\right) \tag{2.29}$$

Figures 2.1 and 2.2 illustrate the physical meaning of $p_t(t-t_i,t_i)$ and $p'_t(t-t_i|t)$: the differences are important, both theoretically and practically, as the former is needed for rainfall-runoff transformations, whereas the latter is what is actually measured by sampling particles at the catchment outlet ([*Rinaldo et al.*, 2011]). Both p_t and p'_t are key descriptors of hydrologic processes, but the role of p'_t becomes prevalent when the main issue is to describe solute transport: in fact, it is able to reconstruct the effects of past rainfall events on the the current chemical composition of discharge depending on the catchment conditions.

Above discussion was devoted to particles exiting the control volume as discharge, but analogously it is possible to define a travel time distribution conditional to exit time for water particles that undergo evapotranspiration, $p'_{et}(t-t_i|t)$. The physical interpretation of p_{et} is analogous to that given for p_t and p'_t respectively, when Q is replaced by ET, as Niemi's theorem can be written also in terms of evapotranspiration flux:

$$J(t_i)\,[1-\theta(t_i)]\,p_{et}(t-t_i,t_i) = ET(t)\,p'_{et}(t-t_i,t) \tag{2.30}$$

2.6 Travel and residence times

In Sections 2.4 and 2.5 analytical expressions for p_t and p'_t for a random sampled storage were derived; analogous results can be obtained following the framework outlined by *Botter et al.*, 2011, whose starting point is the Master Equation for the pdf of residence times, and inserting the mixing hypotesis through the definition of appropriate age functions which fournish

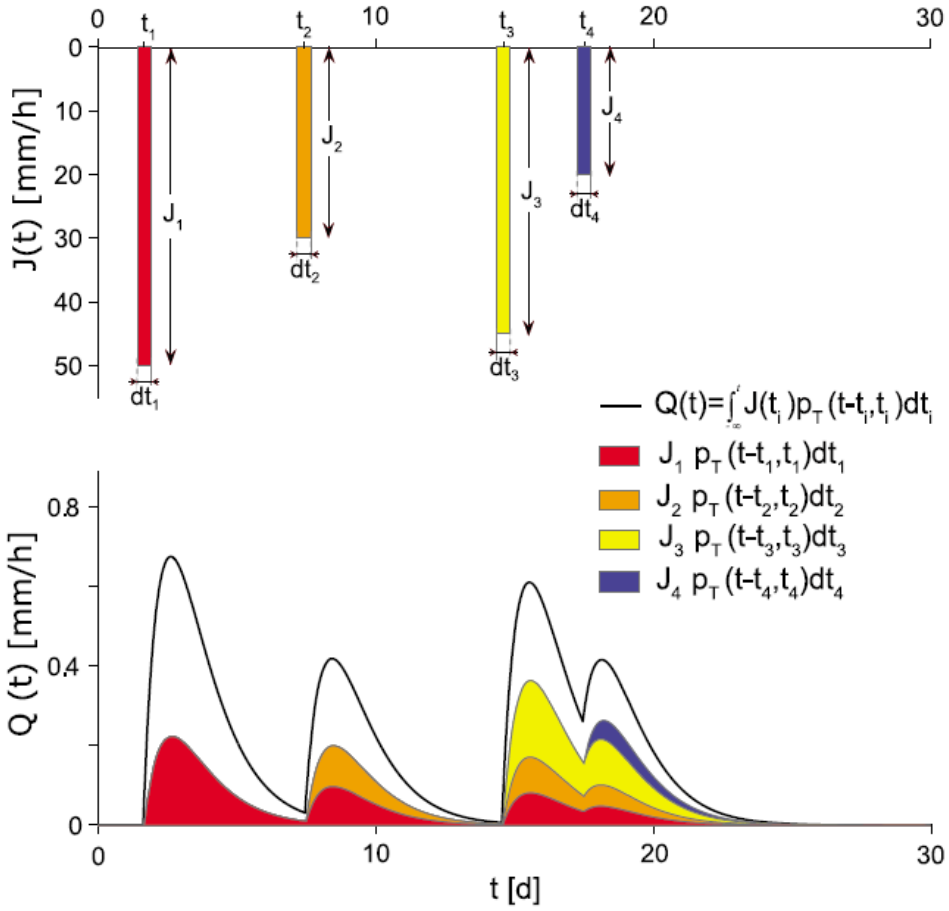

Figure 2.1: *Physical meaning of $p_t(t - t_i, t_i)$ for a fictitiuos sequence of rainfall pulses; ET was neglected for simplicity, i.e. $\theta = 1$. Note that discharge Q at time t is mainly made up of water appertaining to events that came before the event directly related to the peak [picture from Rinaldo et al., 2011].*

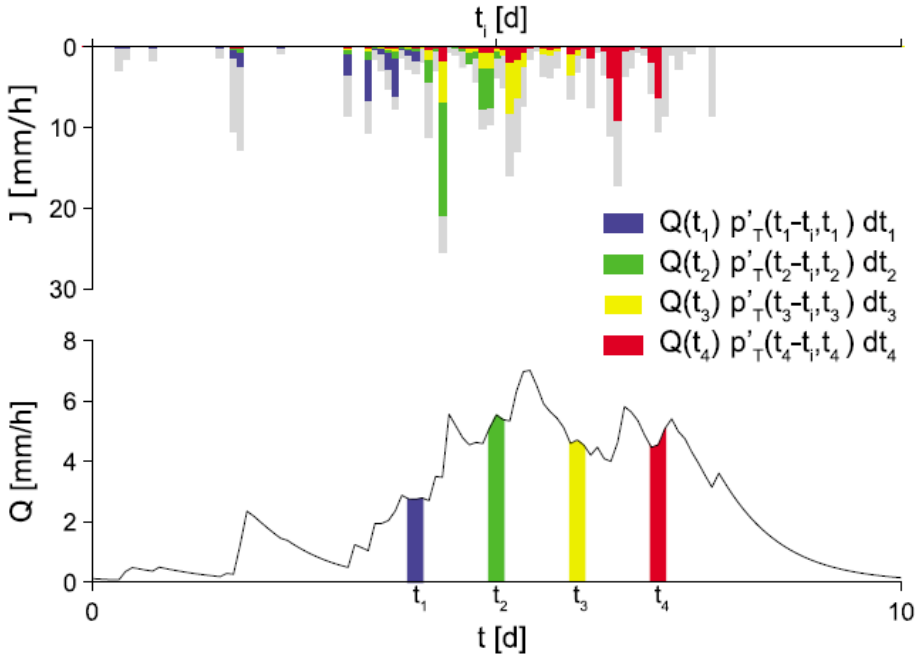

Figure 2.2: *Physical meaning of $p'_t(t-t_i|t)$; ET was neglected for simplicity, i.e. $\theta = 1$. Note that discharge at a fixed time t is made up of water particles injected at different previous times t_i [picture from Rinaldo et al., 2011].*

the linkage between residence and travel times. Finally a relation between the outflowing concentration and concentrations within the storage can be written.

The residence time T_r of a water particle (contained within V at a given time t) is the age of a water particle in the transport volume, i.e. the difference between the current time t and the injection time of the tagged particle: $T_r = t - t_i (t > t_i)$. Residence time is intended as a random variable, whose pdf (evaluated at any possible observation time t) $p_{rt}(T_r, t)$ defines the current ages in storage, that can be used to determine, in a long-term perspective, the persistence of contamination events in the water catchment storage.

The linkage between the age distribution of the water particles stored within the control volume and the travel/evapotranspiration time pdf can be expressed observing that every particle in storage within V tends to increase its age as time progresses. Thus, the uniform aging of the stored particles leads to a linear rightward translation of p_{rt} through time, which can be described by a convective term with unit speed in the positive T_r direction. The output fluxes (ET and Q) also have an impact on the temporal evolution of the residence time pdf, as they determine a subtraction of water particles stored inside V characterized by certain ages, those actually sampled by Q and ET, that are defined by p'_t and p'_{et}. On the contrary, as the age of the rainfall particles at the entrance time is zero, the input rate J does not change the amount of particles stored with $T_r > 0$, but only determines, time by time, the water volume stored with $T_r = 0$. These observations are stated by means of the following Master Equation for the pdf of residence times:

$$\frac{\partial(S(t)p_{rt}(T_r,t))}{\partial t} = -S(t)\frac{\partial p_{rt}(T_r,t)}{\partial t_R} - Q(t)p'_t(T_r,t) - ET(t)p'_{et}(T_r,t) \quad (2.31)$$

The rainfall J leads to a probability flux in $T_r = 0$ expressed by the boundary condition:

$$p_{rt}(T_r = 0, t) = J(t)/S(t) \quad (2.32)$$

The l.h.s. of equation (2.31) expresses the rate of change of the water volume stored in V at time t, which is induced by the aging of resident particles and by the arrivals and ejections. The r.h.s. states that this rate of change is given by the sum of these three terms: the aging of the particles stored in V (first term), the rate of decrease induced by the subtraction through Q and ET of some of the particles stored in V at time t (second and third term, respectively).

Once defined p_{rt} as the pdf of the current ages in storage, and p'_t (and p'_{et}) as the age distribution of the water particle sampled by Q (ET) at a

fixed time t, it is evident that Q (ET) can sample among the ages available in the control volume at that time, that means to state that p'_t (p'_{et}) is always constrained by p_{rt}. The way in which particles are sampled among those in storage is matter of the mixing that is assumed to take place in the soils, thus the relation between travel/evapotranspiration time and residence time is given by a quantity describing those mixing processes:

$$p'_t(T_t, t) = p_{rt}(T_t, t)\omega_Q(T_t, t) \tag{2.33}$$

$$p'_{et}(T_{et}, t) = p_{rt}(T_{et}, t)\omega_{ET}(T_{et}, t) \tag{2.34}$$

Functions ω_Q and ω_{ET} are non-negative, time dependent age functions, which express the affinity of Q and ET with respect to the various available ages. Inserting equations (2.33) and (2.34) into equation (2.31), one gets a first order PDE, which can be solved using the boundary condition (2.32) in terms of p_{rt}, and then, through the age functions and Niemi's theorem, the equations for p'_t, p_t, p'_{et} and p_{et} can be inferred. These general solutions are reported and discussed by *Botter et al.*, 2011,2012.

The assumption of random sampled storage introduced in Section 2.3 can be described by the age functions ω_Q and ω_{ET}: in fact, the random sampled transport volume (where the probability that discharge and evapotranspiration sample particles with a certain age is proportional to their relative abundance within V) can be described setting ω_Q and ω_{ET} constant and equal to 1, leading to the simplification of Master Equation solutions into above equations (2.23), (2.24) and (2.29)and implying the equality $p'_t = p'_{et} = p_{rt}$. Here is that, under the assumption of RS storage, the travel time distribution conditional to exit time can be used in place of the residence time distribution to describe the persistence of solutes within a storage, revealing their prominent role in solute transport decription.

Other mixing hypoteses can of course be contemplated, by means of different age functions: preferential affinities for older/younger water particles can indeed be inserted with time increasing/decreasing age functions.

The solutions of Master Equation can be used to determine the concentration at the outlet of a transported solute, both in the cases of passive and reactive solutes. Solutes are thought to be injected into the system through rainfall with an initial concentration C_J; for passive solutes the input-output relation is:

$$C_Q(t) = \int_{-\infty}^{t} C_J(t_i)\, p'_t(t - t_i, t)\, dt_i \tag{2.35}$$

The RS scheme allows for writing an equivalent expression in terms of p_{rt}, given the equivalence between travel and residence time distributions. Thus the flux concentration in the runoff is given by the composition of the

different water particles' concentrations that are stored within the catchment at any time, yielding:

$$C_Q(t) = \int_{-\infty}^{t} C_J(t_i)\, p_{rt}(t - t_i, t)\, dt_i = \bar{C}(t) \tag{2.36}$$

where $\bar{C}(t)$ is the average storage concentration. This brings notable simplifications in the calculations because the outflowing concentration can now be computed as $\bar{C}(t) = M(t)/S(t)$, where M is the solute mass contained within the storage and can be obtained, as well as S, from a mass balance [*Benettin et al.*, 2013].

For reactive solutes the initial concentration will change in time due to the occurring reactions, and thus the outflowing concentration is function of the actual time t and of the time spent within the catchment T_r, and thus in equations (2.35) and (2.36) the initial concentration C_J must be substituted with the concentration of the outflowing water particles, that can be denoted as $C(T_r, t)$.

2.7 Selective evapotranspiration

Evapotranspiration is a complex process through which plants uptake water from the soil through their roots and then release it as water vapor through their openings located in the leaves (neglecting for simplicity the fraction of water directly transformed into water vapor by solar energy). Considering long-term temporal scales (from seasons to decades) evapotranspiration process plays an important role in the water balance, since it is able to remove from the system significant fractions of the infiltrated water, and at the same time has an effect in the solutes concentrations when dealing with toxic compounds that plant are not willing to take up; in fact, plants perform a selective sampling in the uptaken water, causing an increase of the solute concentration in the stored water.

Plants selectivity is modeled assuming that the concentration of evapotranspiration flux is $\alpha\, C(t - t_i|t)$, where $\alpha \in [0, 1]$ and C is the single value of concentration considered for a RS storage. At every ET sampling an increase in stored concentration takes place since the solutes leave the system at a slower rate than water due to $\alpha \leq 1$, and the increase is quantified by the $(1 - \alpha)$ fraction of concentration that is not uptaken by plants. The increase is described by:

$$\frac{dC(t - t_i|t_i)}{dt} = (1 - \alpha)\frac{ET(t)}{S(t)} C(t - t_i|t_i) \tag{2.37}$$

The water flux driving the process is represented by the ratio $ET(t)/S(t)$ in the r.h.s. of equation (2.37), stating that the expected increase of con-

centration (dC/dt at the l.h.s.) will be greater when the impact of ET on the storage is higher, i.e. during warm periods with lower stored water.

Equation (2.37) is a differential equation that can be solved with the initial condition $C(0|t_i) = C_J(t_i)$ (i.e. initial concentration equal to that entering through rainfall), leading to:

$$C(t - t_i|t_i) = C_J(t_i) \exp\left(\int_{t_i}^{t} \frac{(1-\alpha)ET(x)}{S(x)} dx\right) \tag{2.38}$$

The positive argument of the exponential function at the r.h.s. of equation (2.38) confirms the increase of concentration with respect to the injected concentration, and highlights the dependence of such increase on the full series of ET rates experienced by the impulse from its injection at t_i to present time t, besides the dependence on the specific injection t_i.

Chapter 3

Catchment Description

Plynlimon catchments comprise a set of small catchments located in Mid-West Wales. The area lays within the Cambrian Mountains region, whose highest point is the Plynlimon top (in Welsh Pumlumon Fawr), at 752 m.a.s.l., and it is the source of two big rivers, the Severn (the longest in Britain) and the Wye, flowing down the East side of the massif, then through Wales and England to end into the Bristol Channel. The Upper River Severn (defined by a closure section few kilometers downstream the source) has two main tributaries, the Afon Hafren and the Afon Hore. Between the two is a smaller tributary, the Nant Tanllwyth, which enters the Afon Hafren near its junction with the Afon Hore. Their catchment areas are respectively 3.58, 3.17 and 0.92 km^2 [*Neal et al.*, 2011]. Elevations range from about 300 to 700 m.a.s.l.. The stream here considered is the Hafren, which is further subdivided into two subcatchments: the Upper and the Lower Hafren (see Figure 3.1). The catchments within this area have been studied for about 40 years, resulting in several publications which fully describe its climatic and morphological features [see e.g. *Brandt et al.*, 2004, *Shand et al.*, 2005].

Soil at higher altitudes is mainly composed by blanket peat up to few meters deep, while along hillslopes podzol soils are dominant. Alluvium and gleys dominate the valley parts and the stream channels. The underlying massif bedrock is predominantly composed of fractured Lower Paleozoic mudstones and shales.

Upper Severn catchment has been planted in its lower part with conifers since the 1940s: the trees (mainly Sitka spruce) cover almost the entire Hore and Tanllwyth catchments and the Lower Hafren. Being the trees managed on a forest rotation cycle of about 40 years, the felling of older trees commenced in the 1980s, yielding to the current mix of first rotation forest and of areas that have been felled and replanted with second rotation forest [*Brandt et al.*, 2004]. Upper Hafren vegetation instead comprises semi-natural dwarf shrub heath and bog habitats, representing relatively undisturbed *background* conditions, with minimal recent land use change

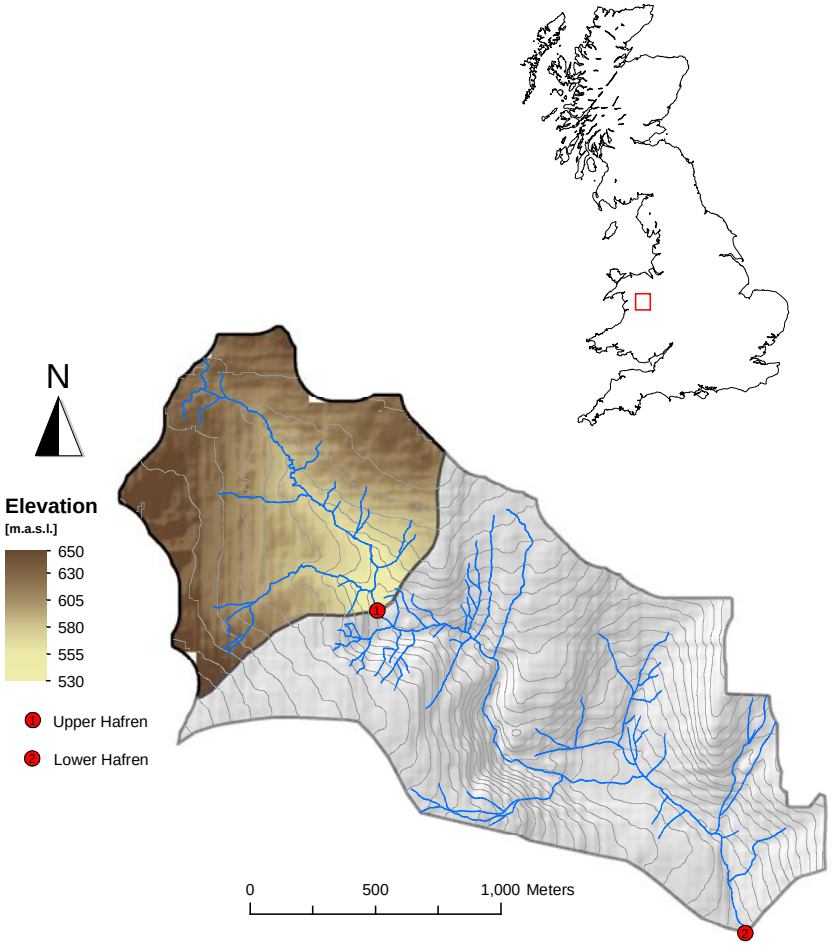

Figure 3.1: *Map of the Upper River Severn catchments [picture by Benettin P.].*

[*Neal et al.*, 2012].

Climate is cool and humid: monthly mean temperatures are tipically 2-3°C in winter and 11-13°C in summer, and annual precipitation is roughly 2500-2600 mm/year, of which approximately 500 mm/year is lost to evapotranspiration and 2000-2100 mm/year runs off as stream discharge. Precipitation varies seasonally, averaging 280-300 mm/month in winter (December/January/February) and 135-155 mm/month in summer (June/July/August). Rainfall frequency is relatively high, with rainy days occurring on about 45% of summer days and over 60% of winter days. Persistent snow cover is rare, then snow contribution to hydrologic response is very small [*Kirchner*, 2009]. Rainfall chemistry is strongly affected by the North Atlantic air masses, that are rich in sea salts: concentrations are highly variable, even within individual storms, with higher concentrations being generally associated with lower rainfall volumes due to atmospheric washout [*Neal et al.*, 2012]. A typical solute that is found in rainfall at relatively high concentrations is chloride, which can be considered a natural conservative tracer due to its characteristics of low chemical and biological reactivity inside the catchment. For this reason its signal can be studied to understand basin hydrological features, such as storage effects, travel and residence times.

Due to the small size of the catchments involved, the response to rainfall inputs is very rapid and intense, with the streamflow peaks occurring rapidly after rainfall events. As shown by *Neal et al.*, 2012, hyrologic and hydrochemical behaviours of Upper and Lower Hafren are similar, reflecting catchments chemical and geological similarities, and the observed differences are mainly due to heterogeneity of land use. The presence of trees in the lower area causes higher concentrations of sea salts, due to enhanced evapotranspiration and atmospheric deposition (through aerosols and cloud water droplets). Borehole observations allowed to detect the movement of water through the fractures [e.g. *Shand et al.*, 2005, *Neal et al.*, 2011], highlighting a high spatial variability in flow and chemistry; it has though seemed clear that groundwater plays a great role in sustaining stream water, especially in dry periods: this fact has been highlighted by the different chemistry observed in stream water and soil water [*Neal et al.*, 1997] and by the groundwater storage effect, used to explain the solutes damped signals recorded in streams with respect to rainfall.

3.1 The data

The british Centre for Ecology and Hydrology (CEH, formerly the Institute of Hydrology) since 1970s has undertaken continuous measurements of precipitation, streamflow and climate characteristics. Precipitation is recorded monthly by a permanent network of rain gauges distributed all over the

area, and hourly by four weather stations (two in Severn catchment, two in Wye), the latter taking in addition measurements of radiation, temperature, wind speed and direction. Streamflow is measured at 15-min intervals in ten sections, comprising the main streams closure sections and those of the main tributaries. Figure 3.2 from *Brandt et al.*, 2004 shows the locations of meteorological and gauging stations all over Plynlimon area.

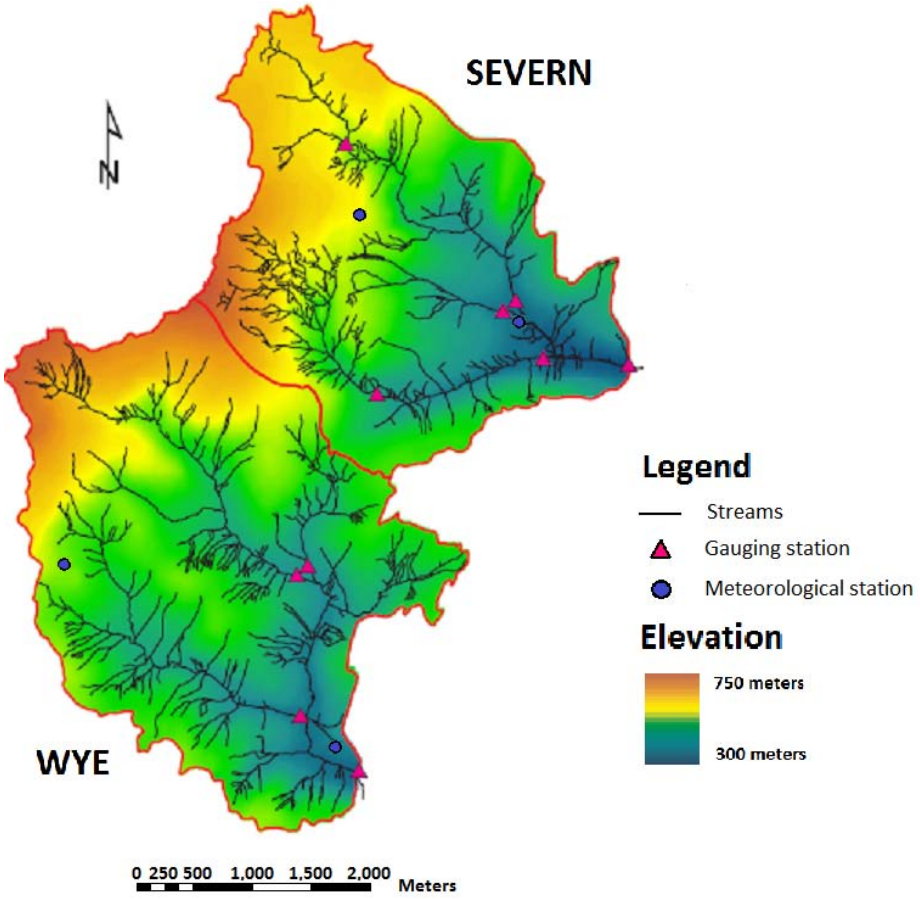

Figure 3.2: *Map of meteorological and gauging stations in Severn and Wye catchments [picture from Brandt et al., 2004].*

Recently, *Neal et al.*, 2012 presented a wide data archive that was made public in 2013 on the CEH Gateway at the Natural Environment Research Council (NERC) Environmental Information Data Centre. The archive includes both high-frequency and long-term series of rainfall and stream water chemistry measurements: eighteen months of 7-hourly data and 20 years of weekly records, respectively.

Early weekly measurements of rainfall and stream water began in May 1983. Afterwards, the monitoring program was progressively made more ex-

tensive including records of cloud water, throughfall, stemflow and groundwater. Instead, sampling operations for high frequency measurements began on 06/03/2007. In Upper Hafren they continued until 27/01/2009, while in Lower Hafren measurements stopped on 11/03/2008. Stream water chemistry was sampled at two sites, Upper Hafren and Lower Hafren, with drainage areas of 1.2 and 3.6 km^2 respectively, while rainfall was sampled at Carreg Wen, at the edge of the Upper Hafren catchment at an altitude of 575 m.a.s.l..

The importance of high frequency measurements is revealed by the evidence that many hydrological processes are characterized by time scales that are typically sub-daily, and then that they cannot be recognized without an appropriate monitoring programme of high temporal resolution. The evidence is even more marked in small catchments, where the hyrologic response has common time scales of few hours. On the other hand high frequency data can not be separated from longer frequency analyses, which have the role of building a general framework of longer time scales processes.

Due to the larger data availability, the present study focuses on Upper Hafren catchment. In addition, due to the presence of some data gaps in the early and late parts of the series, all analyses were limited to a single period spanning approximately 1 year, ranging from December 2007 to November 2008.

Figure 3.3 shows rainfall and discharge measured over the considered period. Rainfall events are quite frequent, with very few dry days; however, within this wet climate context it is possible to observe seasonal changes, with minimum rainfall during May and June, and maximum during October and November. Rainfall events are immediately followed by flow peaks and equally rapid decays characterize times betweeen subsequent events, reflecting the highly responsive nature of the catchment. During the considered period, average flow is $0.13\,m^3/s$, with peaks reaching $1.6 - 1.7\,m^3/s$.

Figure 3.4 shows for the same period the evolution of stream chloride concentration with respect to rainfall inputs: in contrast with figure 3.3, that shows that storm rainfall inputs are usually matched by prompt changes in discharge, streamflow chloride response to storm inputs is strongly damped, indicating that peak flows consist mostly of pre-storm water released from the catchment, rather than rainfall flowing directly into the stream [*Neal et al.*, 1988, *Kirchner et al.*, 2000].

In figure 3.5 stream chloride time series is shown together with the corresponding streamflow. The average concentration during the period is $5.6 mg/l$, with a couple of peaks reaching $10 mg/l$ in January. As highlighted by *Neal et al.*, 2012 it is possible to observe three different behaviours during the year of observations: during the wet period ranging from December to May (defined as Period 1 in Figure 3.5) Cl concentration is highly variable (following the high variability of rainfall and revealing the main contribution of runoff water to streamflow) and has the highest mean ($6.3 mg/l$): the

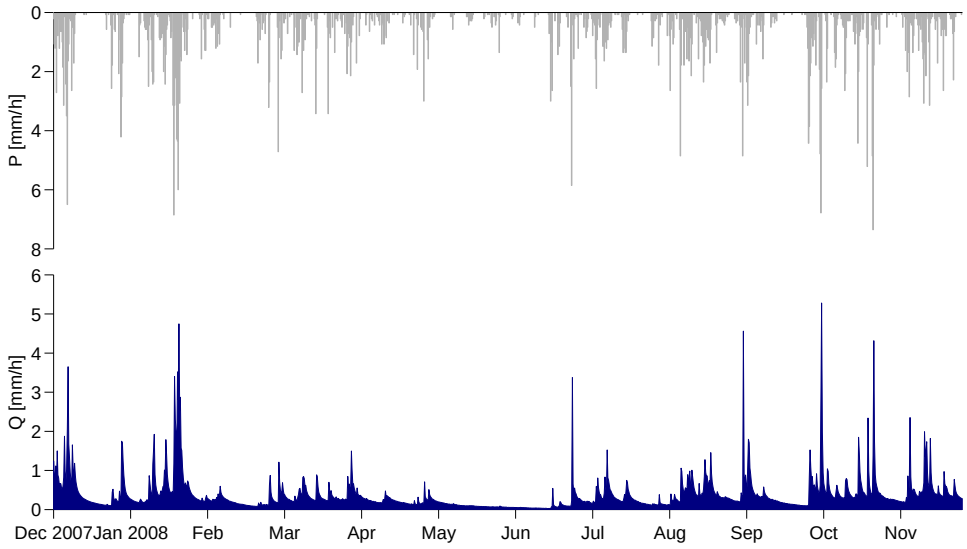

Figure 3.3: *Hydrological flows over the period 01/12/2007 - 30/11/2008.*

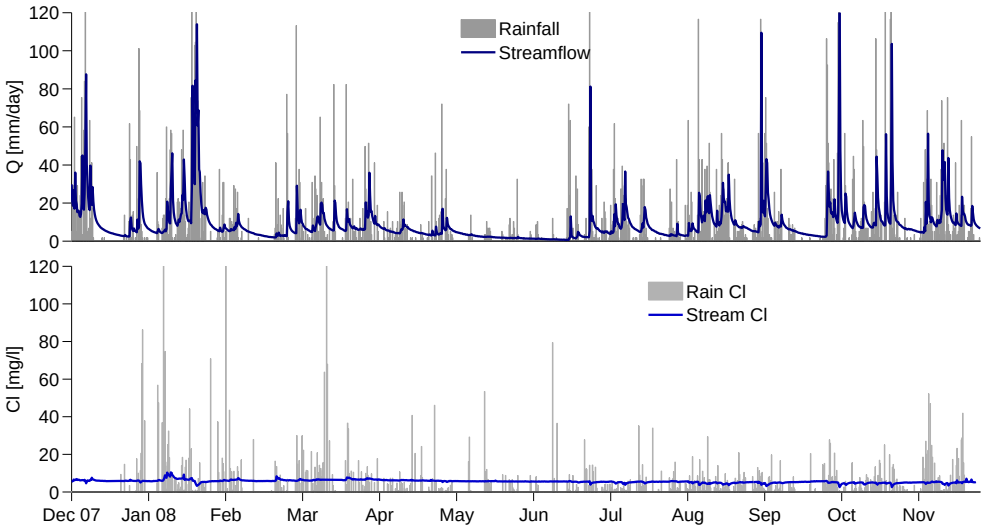

Figure 3.4: *Rainfall and streamflow fluxes (upper) compared to rainfall Cl concentration and stream Cl concentration (lower). Note that stream Cl is highly damped with respect to the input Cl.*

comparison between stream chloride and discharge plots evidences a flushing effect, i.e. at higher streamflows correspond higher Cl concentrations. A different scenario is observed during the dry period ranging from the beginning of May and the first half of June (Period 2), corresponding to a low flow period: Cl concentration in stream is almost constant, reflecting the fact that streamflow is mainly sustained by groundwater. During summer and until the end of November (Period 3), the recurrence of a wet season determines again an high variability of Cl concentration, however with a lower mean (5.0 mg/l) and an opposite effect: at increasing streamflows correspond decreasing Cl concentrations, in a sort of dilution effect.

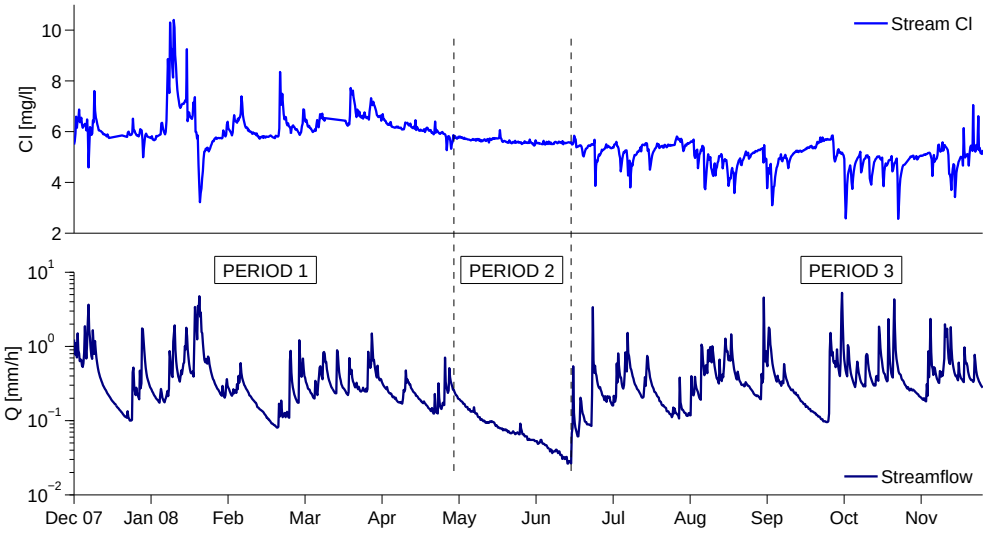

Figure 3.5: *Chloride concentration in streamflow (upper) compared with the corresponding streamflow (lower).*

Chapter 4

Modeling Chloride Concentrations at Plynlimon

The aim of the model is to reproduce both hydrological and chemical response of the Upper Hafren catchment during the considered period (Chapter 3). To this aim, a suitable hydrological model needs to be built, in order to estimate all the involved water fluxes (streamflows, evapotranspiration fluxes, leakages); the generated water fluxes will be the vectors for Cl transport throughout the system, after its entrance through rainfall.

In addition, hydrological model outputs such as soil moisture content s and evapotranspitration ET, together with Q and J, will be further used for travel time distributions calculation.

4.1 Hydrological Model

Upper Hafren catchment is modeled with two overlapping storages: the upper represents the root zone, whose extension is estimable in the first soil's tens of centimeters, and which is responsible of the fast catchment response. Below the root zone is thougt to lay a bigger storage representing groundwater and its slower response. The outputs of these storages contribute to the formation of streamflow together with a third component, represented by the runoff contribution that can be considered as the very fast catchment response.

The root zone water balance is modeled as:

$$nZ_r \frac{ds(t)}{dt} = I(s(t),t) - ET(s(t),t) - L(s(t))$$

where the notation $(s(t),t)$ was adopted to stress the dependence of water flows on soil saturation. Terms in the balance are:

- n : soil porosity $[-]$;

- Z_r : root zone depth $[L]$;
- s : soil moisture content $[-]$;
- I : infiltration $[L/T]$;
- ET : evapotranspiration rate $[L/T]$;
- L : vertical leakage from the root-zone $[L/T]$.

Infiltration is assumed equal to rainfall except for saturated areas, the latter preventing infiltration and thus generating surface runoff. Saturated areas are estimated through a variable contributing areas approach. The fraction of catchment saturated areas is assumed to be function of the root zone saturation by means of a power law of the form $\pi(t) = s(t)^d$. Surface runoff will be then $Q_{sup} = J(t)\,\pi(t)$ and infiltration $I(t) = J(t) - Q_{sup}(t)$.

Actual evapotranspiration was calculated assuming two values for potential ET, corresponding to two periods: a *warm* period, between the 15th of April and the 15th of Semptember, and a *cold* period, during the remaining part of the year; clearly, the value of potential ET during summer period will be greater than that of winter months. These values are assumed to be limited by a stress factor: above a fixed value of saturation s^* evapotranspiration can proceed with its maximum rate, i.e. its potential value. Below s^* evapotranspiration is limited by the water availability: no evapotranspiration is assumed to take place for values of soil saturation lower than the wilting point s_w, and in the interval $[s_w, s^*]$ it is assumed to be a linear function of s.

Leakage from root zone is calculated with Clapp-Hornberger formula [*Clapp and Hornberger*, 1978]: $L(t) = K_{sat}\, s^{2b+3}$; this assumption has the phisical meaning of considering as dominant the gravity driven vertical leaching. A fraction of $L(t)$, namely $a(t)\,L(t)$ reaches the stream channel forming the sub-surface component of streamflow Q_{sub}; the remaining $(1-a(t))\,L(t)$ acts as input for the underlying storage. The partition factor a is time variant and dependent on the soil moisture content according to: $a(t) = a_{sep}\, s(t)$

The equation for groundwater storage water balance is:

$$\frac{dS_{gw}(t)}{dt} = (1-a)L(t) - Q_{gw}(S_{gw}(t))$$

where S_{gw} is intended as a volume of water per unit surface and is measured in mm. The input for groundwater storage is the leakage from the upper root zone. The output flux Q_{gw} is calculated with the assumption of linear reservoir: flux is proportional to the storage through a constant transport coefficient K_{gw}: $Q_{gw} = K_{gw}\, S_{gw}$.

Finally, the discharge reaching the channel is the sum of Q_{sup}, Q_{sub} and Q_{gw}. Q_{sup} is important in better catching the peaks, while Q_{sub} is the most

relevant contribution to streamflow during rainfall events; Q_{gw} instead is responsible for the stream baseflow.

The dependencies of involved terms on water content were expressed, indicating all the model parameters; globally the model comprises 13 parameters: some are reasonably assigned, others need to be calibrated. These parameters are n, Z_r, K_{sat}, b, d, a_{sep}, K_{gw} and the initial values for the storages s_0 and S_0 function of soil characteristics, s_w and s^* function of soil and vegetation, and finally the values of potential evapotranspiration ET_{warm} and ET_{cold} function of climate, vegetation and period of the year.

4.2 Transport Model

The transport model can be set up based on the hydrological model, since the considered conservative solute is thought to be simply advected by water fluxes. The source of Cl for the system is rainfall, whose concentration during the considered period is available in a fairly good number of data.

The main assumption of the transport model is that both root zone and groundwater storages are random sampled. This allows the numerical computation of the outflowing concentrations to be simplified by the introduction of mass balances that implicitly incorporate the time-variant structure of the convolution operations, as shown in equation (2.36) [*Benettin et al.*, 2013]. According to RS hypotesis, flows leaving a storage can be characterized by a single value of concentration equal to the storage mean concentration.

The mass balance for the root zone is modeled as:

$$\frac{dM_s(t)}{dt} = m_I(t) - m_{ET}(t) - m_L(t)$$

The terms represent:

- M_s : chloride mass stored in the root zone $[M/L^2]$;
- m_I : mass flux attached to infiltration $[M/TL^2]$;
- m_{ET} : mass flux attached to evapotranspiration $[M/TL^2]$;
- m_L : mass flux attached to leakage $[M/TL^2]$.

Mass flux associated to infiltration is assumed to have the rainfall Cl concentration, hereafter C_J; its value is obtained multiplying C_J and the infiltration flux given by $I(t) = J(t) - Q_{sup}(t)$. A fraction of Cl mass is supposed to leave the system via surface runoff: $m_{sup} = C_J\, Q_{sup}$.

As chlorides have potential toxicity on plants metabolism [*Taiz and Zeiger*, 2010], it is expectable that a selective sampling in the evapotranspiration takes place. The effect of selective evapotranspiration is taken

into account by means of a parameter α that can vary within the interval $[0, 1]$, and whose value is determined through calibration. Under the hypotesis of random sampling, an average concentration of root zone storage C_s is considered: its value can be calculated by the ratio between the stored mass M_s and the storage specific volume $s\, n\, Z_r$. The mass flux attached to ET is finally calculated as: $m_{ET} = \alpha\, C_s\, ET$.

The term m_L is obtained from the average root zone concentration and the leakage flux: $m_L = C_s L$. This mass is supposed to partition analogously to the water fluxes, i.e. through the partition factor $a(t)$: then, it partially leaves the system through sub-surface flow ($m_{sub} = a(t)\, m_L$) and the remaining part moves downward to the groundwater storage ($(1 - a(t))\, m_L$).

The mass balance for grounwater storage can be written as:

$$\frac{dM_{gw}(t)}{dt} = (1 - a)\, m_L - m_{gw}$$

The only Cl input for underlying storage is the leaked mass from the root zone. The output, instead, is proportional to the average groundwater concentration C_{gw} (obtained again as stored mass M_{gw} divided by the storage volume S_{gw}) through: $m_{gw} = C_{gw}\, Q_{gw}$.

Finally, the stream Cl flux m_Q is obtained as the sum of the three components m_{sup}, m_{sub} and m_{gw}. The modeled stream concentration C_Q is given by the ratio m_Q/Q.

The transport model adds 3 parameters to the hydrological simulation: the selective evapotranspiration factor α and two values for initial concentration in the storages, namely C_{s_0} and C_{S_0}.

A conceptual scheme of the model is shown in Figure 4.1, where the upper and lower storages are visualized and both water and solute fluxes are reported. The model equations concerning the fluxes are summarized in Table 4.1.

A Monte Carlo simulation is performed to calibrate the model: with this approach 10^7 simulations were run with sets of random parameters sampled from credible ranges of values, and for each run the Nash-Sutcliffe model efficiency is evaluated for both hydrological (NS_Q) and transport (NS_C) models with the aim of obtaining the set giving best performances:

$$NS_Q = 1 - \frac{\sum_{i=1}^{N}(Q_{obs} - Q_{mod})^2}{var(Q_{obs})} \tag{4.1}$$

$$NS_C = 1 - \frac{\sum_{i=1}^{M}(C_{obs} - C_{mod})^2}{var(C_{obs})} \tag{4.2}$$

In equations (4.1) and (4.2) N and M are the total number of data for Q and C, respectively; Q_{obs} and Q_{mod} represent the observed and modeled values of discharge for a fixed time instant and analogously C_{obs} and C_{mod} are defined as observed and modeled stream concentrations.

Root zone water balance	$nZ_r \frac{ds(t)}{dt} = I(t) - ET(t) - L(t)$
Infiltration	$I(t) = J(t) - Q_{sup}(t)$
Surface runoff	$Q_{sup}(t) = J(t)\,\pi(t)$
Fraction of saturated areas	$\pi(t) = s(t)^d$
Evapotranspiration	$ET(t) = ET_{pot} \frac{s(t)-s_w}{s^*-s_w}$
Leakage	$L(t) = K_{sat}\, s^{2b+3}$
Sub-surface runoff	$Q_{sub}(t) = a(t)\, L(t)$
Partition factor	$a(t) = a_{sep}\, s(t)$
Groundwater balance	$\frac{dS_{gw}(t)}{dt} = (1-a)L(t) - Q_{gw}(t)$
Groundwater output flow	$Q_{gw}(t) = K_{gw}\, S_{gw}(t)$
Root zone mass balance	$\frac{dM_s(t)}{dt} = m_I(t) - m_{ET}(t) - m_L(t)$
Surface mass flux	$m_{sup} = C_J\, Q_{sup}$
Mass infiltration	$m_I = C_J\, I(t)$
Evapotranspiration mass flux	$m_{ET} = \alpha\, C_s\, ET$
Leaked mass flux	$m_L = C_s\, L$
Sub-surface mass flux	$m_{sub} = a(t)\, m_L$
Groundwater mass balance	$\frac{dM_{gw}(t)}{dt} = (1-a)\, m_L - m_{gw}$
Groundwater mass flux	$m_{gw} = \frac{M_{gw}}{S_{gw}}\, Q_{gw}$

Table 4.1: Summary of model equations.

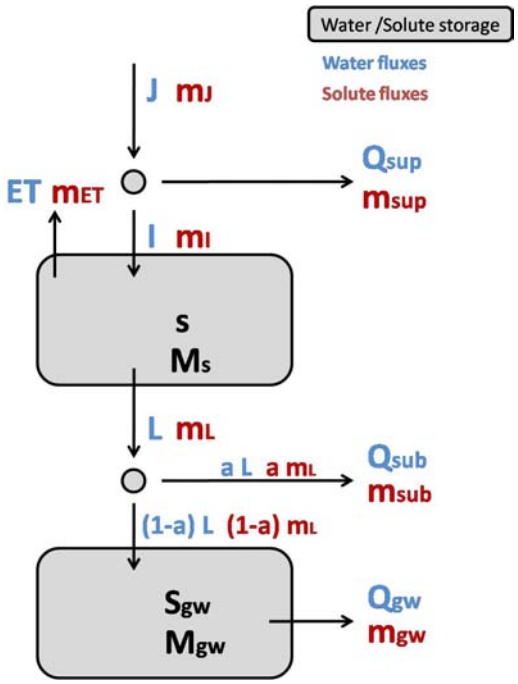

Figure 4.1: *Conceptual scheme of the model.*

Monte Carlo simulation calibrates 9 parameters: b, d, a_{sep}, K_{gw}, S_0, ET_{warm}, ET_{cold}, α and C_{S0}. The remaining 7 parameters (n, Z_r, K_{sat}, s_0, s_w, s^* and C_{s0}), instead, are reasonably assigned. The final set of parameters is reported in Table 4.2: Nash-Sutcliffe efficiency shows that the model is in general reliable in reproducing the measurements, both for discharge (NS=0.82) and chloride concentration (NS=0.35).

parameter	*symbol*	*value*	*unit*
soil porosity	n	0.3	–
root zone depth	Z_r	300	mm
saturated soil conductivity	K_{sat}	100	cm/d
Clapp-Hornberger parameter	b	9	–
variable contributing areas exponent	d	19	–
fraction of drained leakage	a_{sep}	0.8	–
groundwater transport coefficient	K_{gw}	$3.2\,10^{-4}$	h^{-1}
initial root zone saturation	s_0	0.8	–
initial groundwater storage	S_0	380	mm
soil moisture at wilting point	s_w	0.1	–
soil moisture for ET stress	$s*$	0.4	–
potential ET during hot period	ET_{hot}	0.02	mm/h
potential ET during cold period	ET_{cold}	0.01	mm/h
plants selectivity constant	α	0.7	–
initial root zone Cl concentration	C_{s0}	10	mg/l
initial groundwater Cl concentration	C_{S0}	5	mg/l

Table 4.2: Parameters of the model.

Chapter 5

Results

The results of the simulation are here presented and examined to individuate model strenghts and weaknesses, trying to assess the its global robustness beyond the value of Nash-Sutcliffe coefficients reported in Chapter 4.

Figure 5.1 shows the whole calculated time series compared with the measurements. The comparison between the simulated streamflow and measured data reveals that the model is generally able to reproduce the observed streamflow, detecting almost all the peaks that follow rainfall events, even if the highest peaks are little overestimated (in December 2007, and two between September and October 2008), and the lower spring-summer peaks little underestimated. It is to observe also a slight overestimation of the signal during the relatively dry days of May and the first half of June.

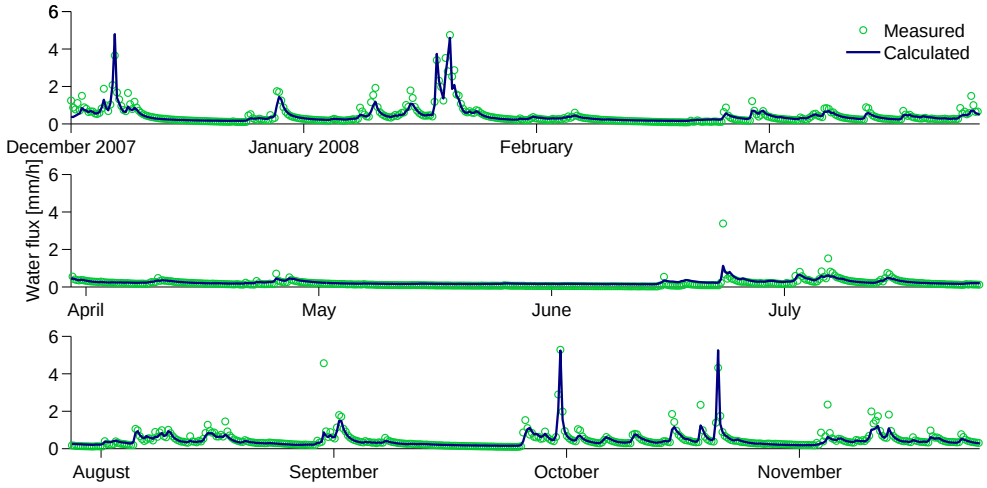

Figure 5.1: *Calculated vs Measured Upper Hafren discharge.*

Model performance can be assessed also through the computation of the

cumulative curves of measured and calculated discharge (Figure 5.2). The comparison between the cumulative curves shows an optimal behaviour, with slightly under and overestimations yielding to a final good correspondence in outflowing volumes.

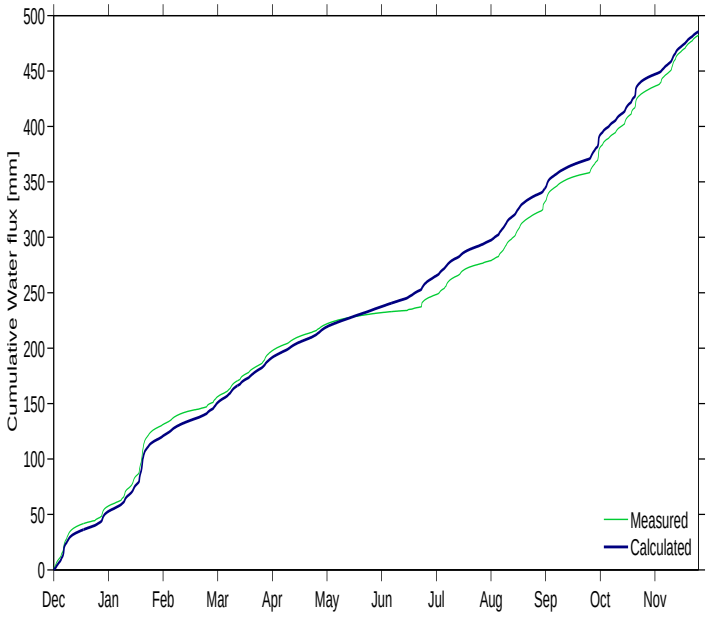

Figure 5.2: *Cumulative comparison between measured and calculated streamflows.*

In Figure 5.3 modeled hydrological flows are reported; it is noteworthy that the very humid climate is reflected in the root zone moisture, that is always higher than 0.7, reaching values of 0.9 and with a mean value during the period of 0.79. The soil moisture is the main factor influencing evapotranspiration: being the value of s always higher than the stress point ($s^* = 0.4$) evapotranspiration proceeds with the potential rates ET_{warm} from mid-April to mid-September, and ET_{cold} during the remaining months, resulting in the step-shaped ET plot in Figure 5.3. Due to the vegetation cover present in Upper Hafren catchment, mainly consisting in low-height shrubs, the potential ET values are low, and consequently evapotranspired water volume represents only the 4% of total infiltrated water.

The total simulated flow is separated into its three contributions, coming from the surface runoff, the subsurface flow and the groundwater; the aim is to give confirmation to the assumptions made in Chapter 4, trying to understand the relative importance of each flow during different periods and rainfall amounts. Figure 5.4 shows the flow contributions. Q_{sup} represents

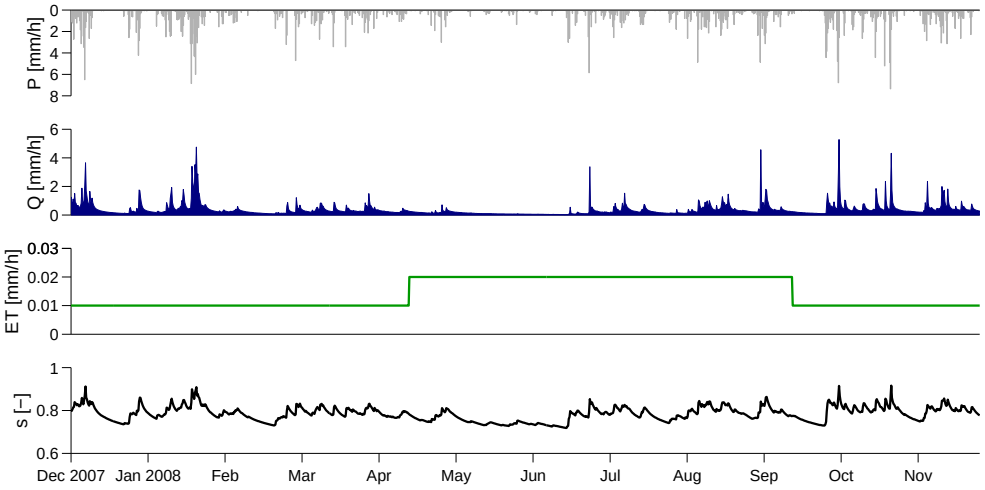

Figure 5.3: *Calculated Upper Hafren hydrological flows.*

a very little fraction of total discharge (less than 3% during the period), but it is responsible for the formation of peak discharges, and particularly relevant in the few highest peaks. Q_{sub} is the most important contribution, representing the approximately 65% of total flow; its behaviour is very variable, clearly following the high variability of rainfall. Conversely Q_{gw} (32% of total discharge) remains almost constant during the period, showing to be very little or none affected by rainfall events; its relative importance increases during inter-events time, when it becomes the main source mantaining the stream baseflow.

The results of chloride transport modeling are reported in Figures 5.5 and 5.6. The behaviour of Cl signal in Upper Hafren stream is globally captured, particularly in the first part of the series (Periods 1 and 2, with reference to Figure 3.5); in the last part, instead, a diffuse underestimation of observed data is obtained. However, the overall dynamics of the chemical signal are well reproduced, as the model is able to detect the sequence of upper and lower peaks, possibly meaning that the chloride signal is sustained by an alternative source, that could be an underlying very slow groundwater storage. However, globally the result can be considered satisfying.

As already done for the stream discharge, the different contributions of root zone and groundwater to the stream chloride signal are separated. Figure 5.6 shows these contributions. It is evident that the stream Cl is given by the flux weighted average of the concentration transported by the subsurface flow and that transported by groundwater. However, it is noticeable that in the first part of the simulation the main contributor is the root zone Cl, that is systematically higher than the deep Cl, but at a certain time (little

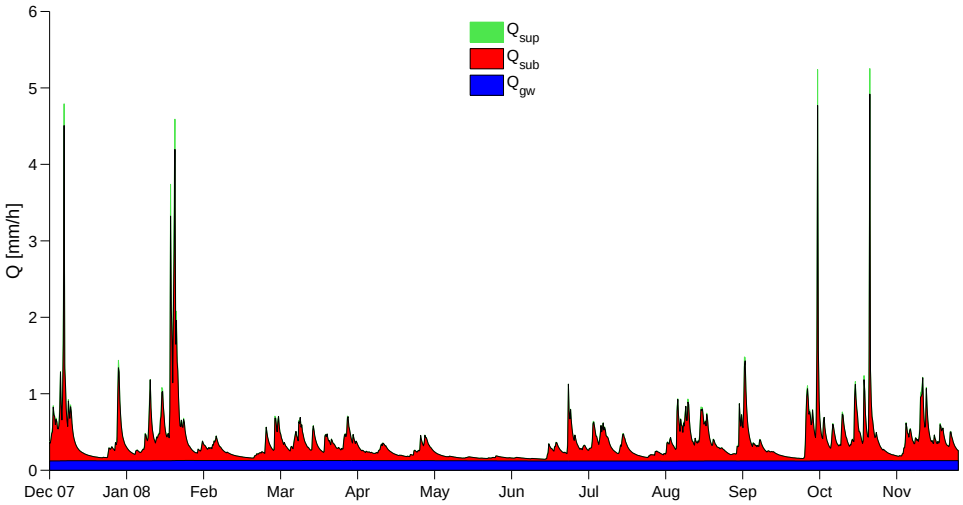

Figure 5.4: *Calculated flow contributions.*

after the beginning of Period 3, see figure 3.5) an inversion occurs, with the deep storage concentration becoming higher than the root zone concentration. This evidence can possibly explain the different behaviours of stream Cl concentrations discussed in Chapter 3. The key point is identified in the rainfall concentration: when the input concentration is sufficiently high it is able to influence the whole root zone increasing its overall concentration and consequently the concentration in streamflow, giving rise to the behaviour observed during Period 1 (mean rainfall concentration: 14.6 mg/l); on the contrary, if rainfall concentration is not high enough it will not significantly affect the concentration in the root zone, and then the exiting flow will tend to dilute the streamflow, as observed during Period 3 (with a mean rainfall concentration of 6.5 mg/l).

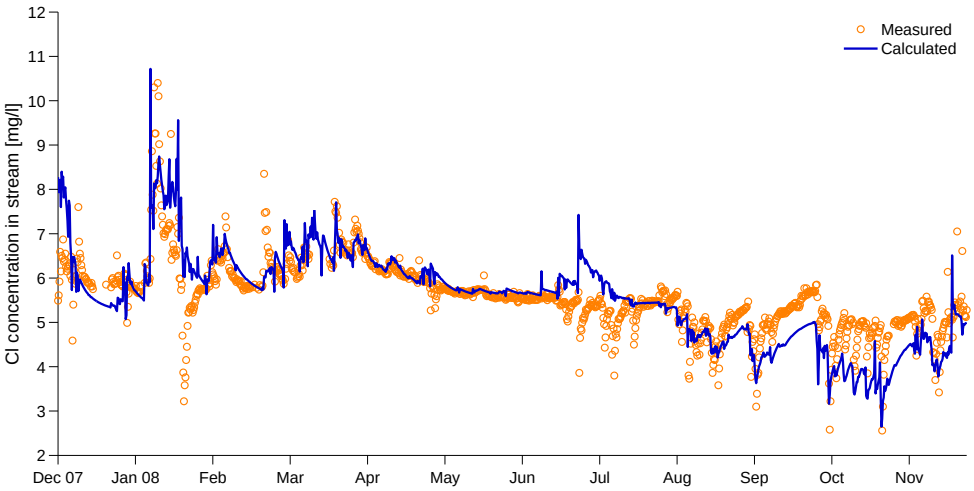

Figure 5.5: *Calculated vs Measured Upper Hafren chloride concentration.*

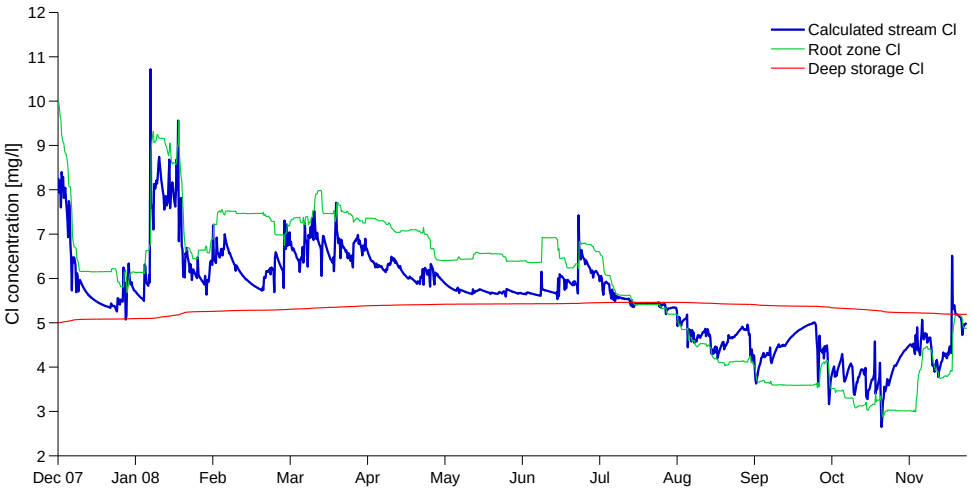

Figure 5.6: *Calculated stream chloride contributions.*

Chapter 6

TTDs Calculation

Rainfall data, together with the outputs of hydrological model (water flux, evapotranspiration and soil moisture), are further exploited to calculate the Travel Time Distributions for water and solutes, according to the theoretical development outlined in Chapter 2. The calculation is made either for fixed injection and exit time excluding the last days of the simulation for the former, and first for the latter, in order to focus the attention on those specific injections/exits. Travel times computation is only performed for the upper and faster storage: in fact, root zone response times typically range from some days to few weeks, and then the considered time window is large enough to fully catch root zone dynamics. Conversely, groundwater storage exhibits slower response times, typically of the order of months, that cannot be fully catch by the year of simulation.

Figures 6.1 and 6.2 show two examples of TTDs conditional to injection time taken during the first months of the simulation (from December 2007 to April 2008); to emphasize the time-dependent nature of travel times, injections are intentionally choosen during periods with different catchment conditions. In Figure 6.1 injection time t_i is fixed right before a period of relatively high precipitation and corresponding high flows: the pdf shows that the injection is almost fully released in about 20 days, with a mean of the pdf, representing the average time to leave the system, of 17 days. In addition, pdf's shape suggests that water particles entered in the system at t_i are most released during streamflow peaks following t_i, proportionally to the magnitude of the event and with decreasing importance as time proceeds from the injection, due to the progressive removal of particles via Q and ET. On the contrary, the removal of particles from the system takes longer times during relatively dry periods, as shown in Figure 6.2; the shape of pdf is again resembling the sequence of streamflow peaks, confirming the dependence of travel times on streamflow evolution after the injection, but releasing times much higher with respect to the previous situation, with a mean travel time of 37 days and the almost full release of the particles in

about 90 days.

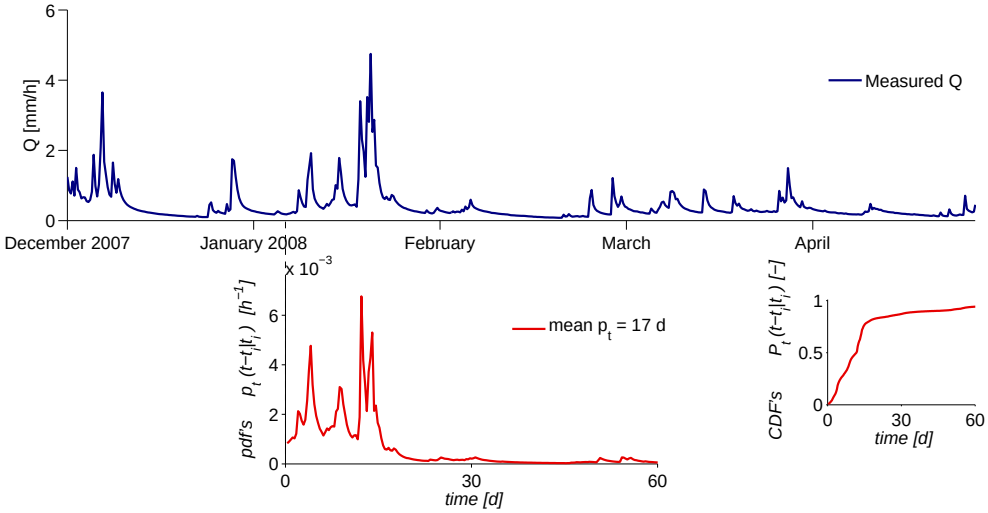

Figure 6.1: *Example of TTD conditional to injection time for a time instant preceding a wet period. The lower right plot shows the corresponding cumulative probability.*

Figures 6.3 and 6.4 compare p_t and p_{et} for the same injection, suggesting the marginal role played by evapotranspiration exiting flow with respect to discharge flow, due to the climate and the type of vegetation cover observed in the catchment. Figure 6.3 refers to the same rain injection of Figure 6.1, representing an event taking place at the beginning of January, during the *cold* months (as defined in Chapter 4), just before a period characterized by intense rainfall: the value of θ, which expresses the fraction of injected water released as streamflow (reported in the upper part of the plot), is 0.96, meaning that only a very little fraction of water is evapotranspired, in accordance with the cold-wet climate of the period. Mean travel and evapotranspiration times are similar (17 and 14 days, respectively) but the behaviours of p_t and p_{et} are very different: p_t keeps track of the succession of streamflow peaks coming after the injection, while p_{et} seems to be noway influenced by streamflow peaks, only showing a time-decreasing behaviour due to the decreasing rate of removal of solute particles. A different scenario is instead presented in Figure 6.4, showing p_t and p_{et} for an injection at the beginning of May preceding a dry period, and within the *warm* months: mean travel times increase to 52 days for p_t and 31 for p_{et}, with tails of the distributions reaching 90-100 days; the value of θ, albeit decreased to 0.87, still remains very high, showing that even during warm-dry periods discharge flow is predominant with respect to evapotranspiration.

Two examples of TTDs conditional to exit time are shown in Figures 6.5 and 6.6, choosing again two time instants that could represent opposite

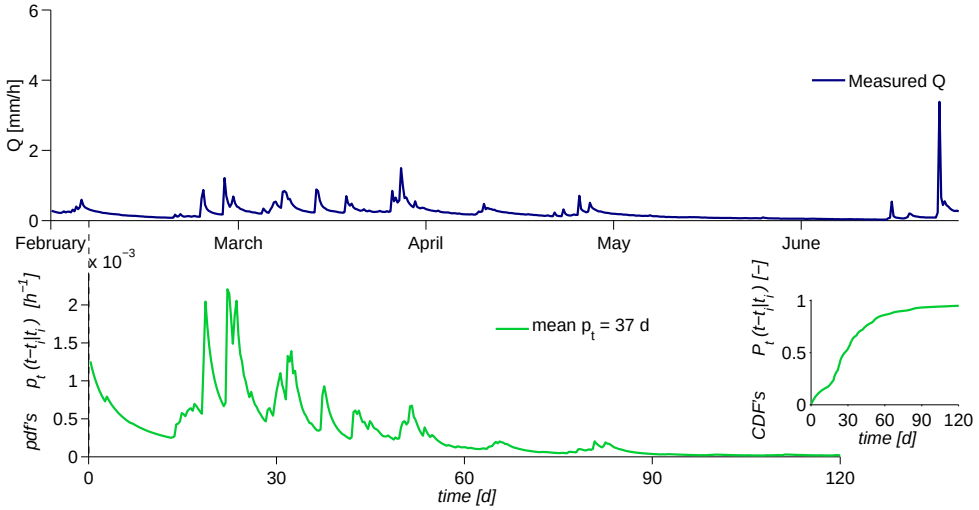

Figure 6.2: *Example of TTD conditional to injection time for a time instant preceding a dry period. The lower right plot shows the corresponding cumulative probability.*

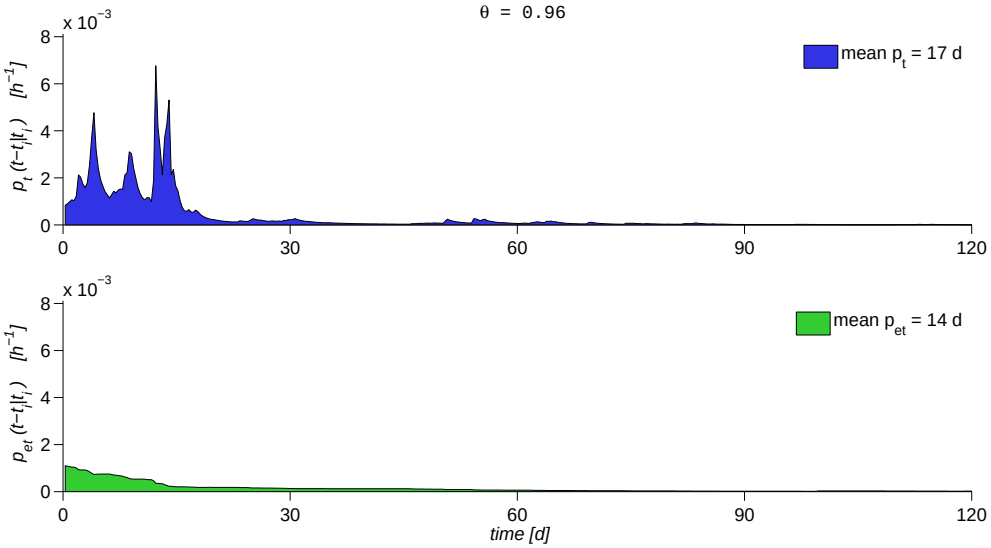

Figure 6.3: *Comparison of p_t (upper plot) and p_{et} (lower) for a cold-wet period.*

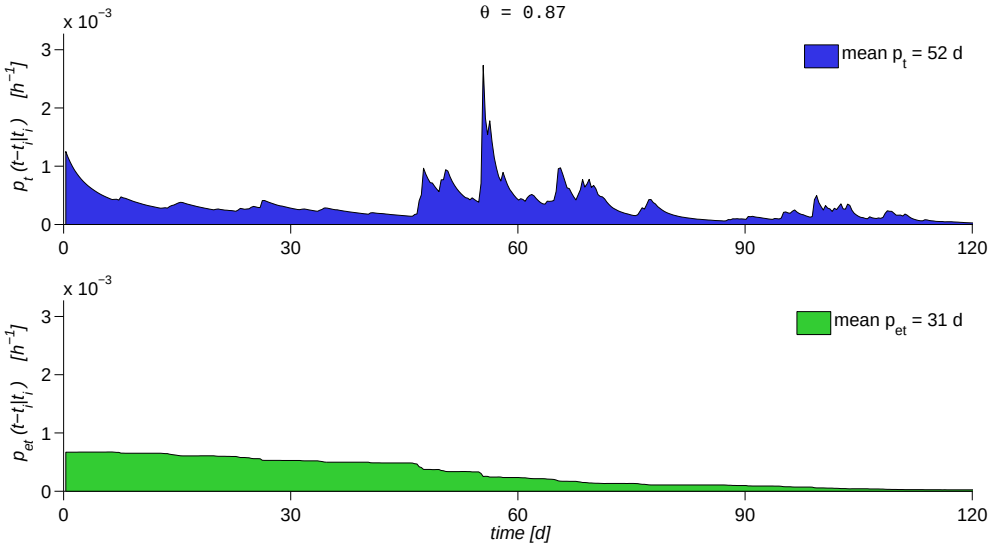

Figure 6.4: *Comparison of p_t (upper plot) and p_{et} (lower) for a warm-dry period.*

catchment conditions. The exit time selected in Figure 6.5 comes at the end of a wet with enhanced rainfal,l and this condition is reflected by the pdf of p'_t: bars are compressed in the right part of the plot, revealing that sampled water ages are relatively young with a mean p'_t of 22 days, with little probability for water ages exceeding 30 days. Figure 6.6 indicates a higher pdf mean of 63 days and relevant probabilities for water ages up to 90 days, as the exit time was fixed after a dry period without any rainfall event for almost one week. The upper plots show the precipitation inputs (during the first part of the simulation, from December 2007 to March 2008): it is noteworthy that the TTDs conditional to exit time are strictly reflecting rainfall dynamics preceding the sampling time.

The time-dependence of TTDs is further pointed out in Figure 6.7, which shows the mean travel times corresponding to each injection of the period, excluding the injections taking place in the last two months of the simulation (October and November 2008), whose release from the system will significantly exceed the simulation time. The variation of mean travel time with respect to the average over the period, that is 30 days, is quite wide and follows an overall seasonal trend, reaching the highest values (up to 52 days) in the central part of the simulation, i.e. during the dry period, and falling to the lower values of 15-20 days during wetter months of January and October-November. Similar plots can be obtained considering the mean travel times conditional to exit time (Figure 6.8) for all the simulation time instants, with the exception of the first two months (December 2007 and January 2008), in order to exclude those sampling times mainly constituted

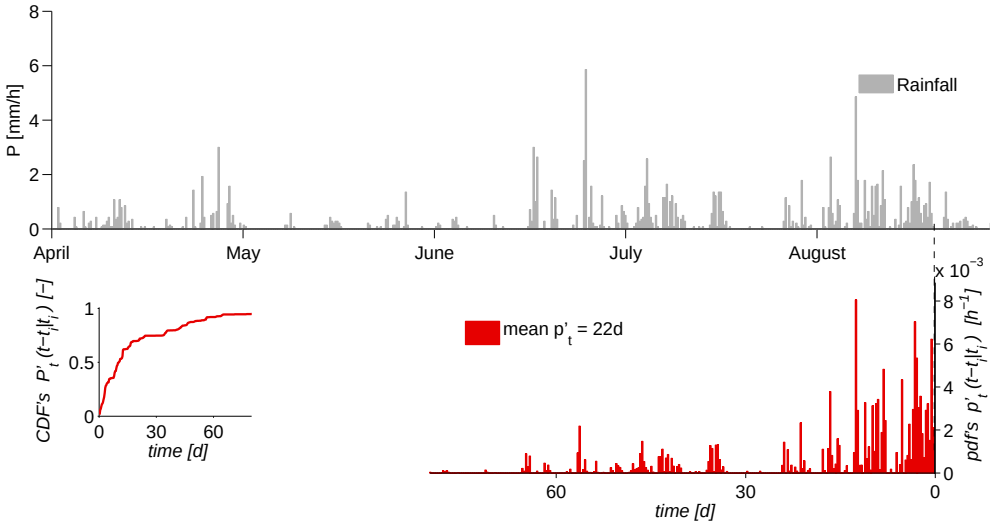

Figure 6.5: *Example of TTD conditional to exit time for a time instant following a wet period. The lower right plot shows the corresponding cumulative probability.*

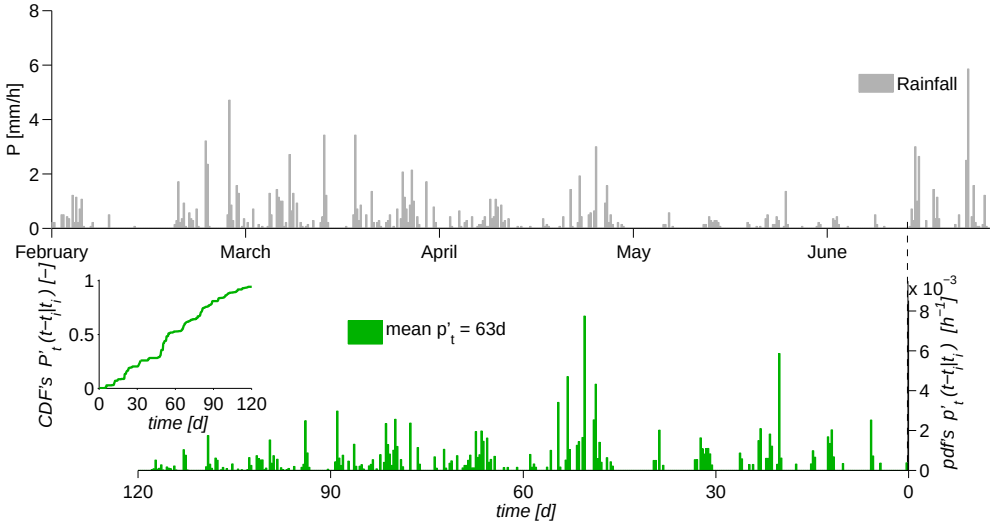

Figure 6.6: *Example of TTD conditional to exit time for a time instant following a dry period. The lower right plot shows the corresponding cumulative probability.*

by water that entered the system before the simulation time. The average travel time over the period is 31 days, very similar to that previously obtained, and again a seasonal trend is recognizable over the event-scale fluctuations: in fact, the decrease in mean travel time occurs in correspondence to rainfall events, that cause the entrance of new water particles into the system, while in between the events a linear increase is observed, due to the aging of the present particles. The difference with the previous figure relies on the more frequent and less pronounced fluctuations observed in the pdfs conditional to the exit time; this behaviour reflects the different dynamics the travel times are related to: p'_t reproduces faster and more frequent variations in rainfall, while p_t follows the dynamics of streamflow, which are modulated by the storage of the catchment.

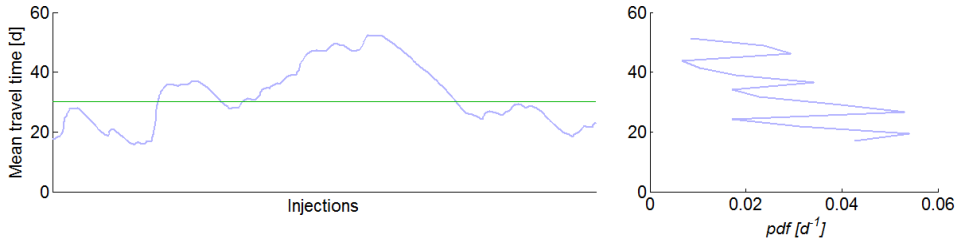

Figure 6.7: *Variation of mean travel time conditional to injection time during the simulation and average mean travel time over the period (left). Pdf of mean travel time conditional to injection time (right).*

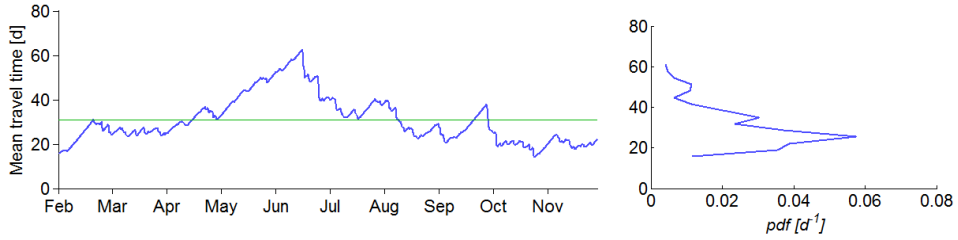

Figure 6.8: *Variation of mean travel time conditional to exit time during the simulation and average mean travel time over the period (left). Pdf of mean travel time conditional to exit time (right).*

Chapter 7

Discussion

Reliable hydrological models for a small catchment within Plynlimon area have been developed and examined. This result is gained through a model that makes simplicity its strenght: the number of parameters is limited and their clear physical meaning is functional to the calibration procedure, since it provides a costrain to the range explored. Chloride signal is deemed to be satisfactorily modeled, given the complexity of the issue, allowing a deeper understanding of involved processes. The variability of inputs and system responses during the year of observations has been properly captured. Moreover, (following *Page et al.*, 2007), the study leaves open the question whether *occult* sources of chloride that are not taken in account in the mass balance, comprising dry deposition, cloud droplet deposition and fluxes due to inputs come prior to the study period are actually a major process. Indeed, estimates of such contributions and their relevance at medium-large temporal scales are prevented by the lack of longer-term data.

The model consists of two overlapping random sampled storages, that can be representative of a catchment where subsurface heterogeneity dispersion favor water mixing. The validity of the mixing hypotesis, despite its simplicity, is confirmed by model performances, as in a double-storage scheme the non-linear and non-stationary relationship between the storages result in a non-randomly sampled overall system. It is clear that the system could be differently modeled, in terms of number of storages and mixing hypoteses. It has been already experienced [see e.g. *Bertuzzo et al.*, 2013, *Benettin et al.*, 2013] that a single storage scheme is able to reproduce discharge series with the same accuracy of a double-storage model, but the roughness of such a model prevents for a satisfactory modeling of solutes, that can be captured only through a more subtle description of the catchment, separately accounting for fast and slow contributions. Furthermore performances could potentially be enhanced by the inclusion of more storages, for example to differentiate among groundwaters. Concerning mixing

hypotesis, other schemes could be tested and combined among storages to gain better results, such as piston flow like models producing the preferential release of old water [see e.g. *Botter*, 2012], preferential flowpath models leading to the preferential explusion of new water [see e.g. *Botter et al.*, 2009] or other more complex threshold-based schemes, where the percentage of new/old water released during a given event depends on the actual soil water content and the underlying hydrologic conditions [*Botter et al.*, 2010]. In any case, it is to verify if the increase of the number of parameters, that is necessary implementing sophisticated schemes with more storages and more complex mixing hypoteses, is enough convenient in terms of improved model performances.

Catchment travel time pdf's have often been assumed to be simple, time-invariant pdf's, such as exponential or gamma functions [see, e.g. *Maloszewski and Zuber*, 1982, *McGuire and McDonnell*, 2006]. Recent works [*Botter et al.*, 2010, *Duffy*, 2010] have instead suggested that travel time pdf's must be time-variant to reflect the variability of the rainfall forcings and the related hydrologic dynamics [*Botter et al.*, 2011]. Simulation performed at Plynlimon firmly confirms the time-variance of travel time pdfs, in response to the fluctuations of climatic conditions and rainfall events affecting soil moisture and streamflow dynamics. A comparison between three travel time distributions evaluated at three different injection times is shown in Figure 7.1, and the same comparison is shown for three different exit times in Figure 7.2: the differences among the curves are evident, reinforcing the inappropriateness of stationary descriptions of transport dynamics.

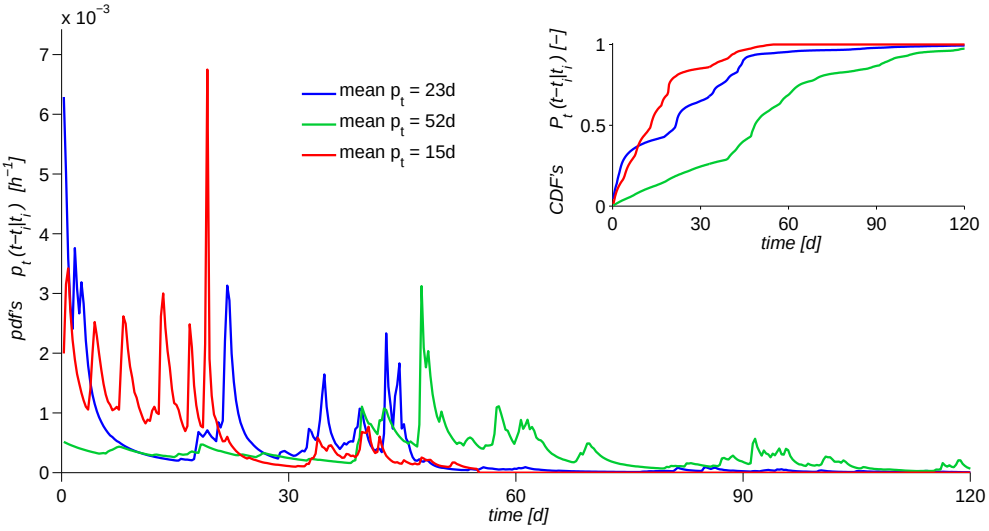

Figure 7.1: *Three examples of TTDs conditional to injection time (big plot) and their cumulative curves (small plot).*

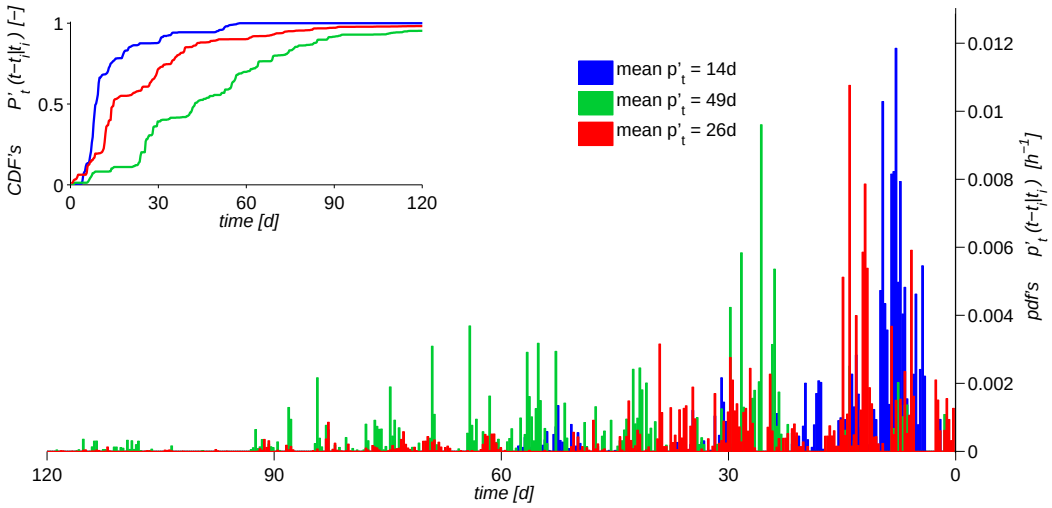

Figure 7.2: *Three examples of TTDs conditional to exit time (big plot) and their cumulative curves (small plot).*

Due to the short available time series, the calculation of TTD's for the groundwater storage was not performed in the present work, but some remarks could anyway be made: the analytical dependence of p_t on S (equation (2.23)) evidences that travel times grow with storage dimensions in a non-linear way, confirming the ansatz that a bigger storage should receive an higher number of particles that would spend longer times in the system, resulting in a huge variability of stored ages. It is expectable, then, that the mean travel time for groundwater will grow with respect to that calculated for root zone (that is of the order of tens of days), and that the bigger storage will be not affected by single rainfall events, but rather by seasonal climatic fluctuations.

Chapter 8

Conclusions

The scheme set up to model hydrological flows and chloride transport within Upper Hafren catchment proved to be effective for both the purposes. The double-storage scheme employed in this study allows for the separate detection of fast and slow responses, whose relative contribution to streamflows was shown to be highly variable depending on the succession of relatively wet and dry periods; such a separation is identified as the key process in describing stream chloride concentrations at Plynlimon, whose dynamics are ultimately determined by the combination of a contribution from the upper storage (influenced by single events), and a contribution from the groundwater (event-independent).

The presented theoretical framework concerning travel time distributions was successfully applied, highlighting the strong time-dependent nature of catchments responses, and the consequent roughness of stationary approaches. In particular, the study evidenced that the release of water from the root zone is driven by rainfall events following the injection: under wet Plynlimon climate this fact implies the fast renewal of waters and the consequent fast release of solutes. The persistency of compounds within soils is indeed strictly linked to climate features, beyond the characteristics of the solute itself and the physical properties of subsurface environments. The great advantage of describing solute and water fluxes in heterogeneous media is the lumped nature and the generality. No restrictive assumptions have to be made in defining the model structure, so that it can be throughout applied based on water flows estimates and a suitable mixing scheme.

Concerning research improvements, within the Plynlimon area it would be significant to integrate the present work by testing the chloride model over longer periods, allowing for a proper calculation of travel time distributions for the groundwater storage. To this aim the twenty years of weekly observations of chloride concentrations that are readily available could be employed. Parallel, the description of the dynamics of other solutes could be undertaken within the same framework, including reactive solutes that

undergo transformations within soils for which mass balance and reactive terms should be included in the formulation. Furthermore, different mixing schemes could be tested to determine site-specific mixing schemes by means of measurement and analysis of water fluxes and solute concentrations within the study catchment.

Bibliography

[1] Benettin, P., van der Velde, Y., van der Zee, S.E.A.T.M., Rinaldo, A. and Botter G. (2013), Chloride circulation in a lowland catchment and the formulation of transport by travel time distributions, *Water Resour. Res.*, 49, doi: 10.1002/wrcr.20309.

[2] Bertuzzo, E., Thomet, M., Botter, G. and Rinaldo, A. (2013), Catchment-scale herbicides transport: Theory and application, *Adv. Water Resour.*, 52: 232-242, doi: 10.1016/j.advwatres.2012.11.007.

[3] Botter, G., Bertuzzo, E., Bellin, A. and Rinaldo, A. (2005), On the Lagrangian formulations of reactive solute transport in the hydrologic response, *Water Resour. Res.*, 41, W04008, doi: 10.1029/2004WR003544.

[4] Botter, G., Milan, E., Bertuzzo, E., Zanardo, S., Marani, M. and Rinaldo, A. (2009), Inferences from catchment-scale tracer circulation experiments, *J. Hydrol.*, 369(3-4): 368-380, doi: 10.1016/j.hydrol.2009.02.012.

[5] Botter, G., Bertuzzo, E. and Rinaldo A. (2010), Transport in the hydrologic response: Travel time distributions, soil moisture dynamics, and the old water paradox, *Water Resour. Res.*, 46, W03514, doi: 10.1029/2009WR008371.

[6] Botter, G., Bertuzzo, E. and Rinaldo, A. (2011), Catchment residence and travel time distributions: The master equation, *Geophys. Res. Lett.*, 38, L11403, doi: 10.1029/2011GL047666.

[7] Botter, G. (2012), Catchment mixing processes and travel time distributions, *Water Resour. Res.*, 48, W05545, doi: 10.1029/2011WR011160.

[8] Brandt, C., Robinson, M. and Finch, J.W. (2004), Anatomy of a catchment: the relation of physical attributes of the Plynlimon catchments to variations in hydrology and water status, *Hydrology and Earth System Sciences*, 8: 345-354.

[9] Clapp, R.B. and Hornberger G. M. (1978), Empirical equations for some soil hydraulic properties, *Water Resour. Res.*, 14(4): 601-604, doi: 10.1029/WR014i004p00601.

[10] Duffy, C. (2010), Dynamical modelling of concentration-age-discharge in watersheds, *Hydrol. Processes*, 24: 1711-1718, doi: 10.1002/hyp.7691.

[11] Kirchner, J.W., Feng, X. and Neal, C. (2000), Fractal stream chemistry and its implications for contaminant transport in catchments, *Nature*, 403: 524-527, doi: 10.1038/35000537.

[12] Kirchner, J.W. (2009), Catchments as simple dynamical systems: Catchment charachterization, rainfall-runoff modeling, and doing hydrology backward, *Water Resour. Res.*, 45, W02429.

[13] Maloszewski, P. and Zuber, A. (1982), Determining the turnover time of groundwater systems with the aid of environmental tracers: 1. Models and their applicability, *J. Hydrol.*, 57: 207-231.

[14] McGuire, K.J. and McDonnell, J.J. (2006), A review and evaluation of catchment transit time modeling, *J. Hydrol.*, 330: 543-563, doi: 10.1026/j.hydrol.2006.04.020.

[15] Neal, C., Christophersen, N., Neale, R., Smith, C.J., Whitehead, P.G., Reynolds, B. (1988) Chloride in precipitation and streamwater for the upland catchment of the River Severn, mid-Wales: some consequences for hydrochemical models, *Hydrol. Processes*, 2: 155-165.

[16] Neal, C., Wilkinson, J., Neal, M., Harrow, M., Wickham, H., Hill, L. and Morfitt, C. (1997), The hydrochemistry of the headwaters of the River Severn, Plynlimon, *Hydrol. Earth Syst. Sci.*, 1: 583-617.

[17] Neal, C., Reynolds, B., Norris, D., Kirchner, J.W., Neal, M., Rowland, P., Wickham, H., Harman, S., Armstrong, L., Sleep, D., Lawlor, A., Woods, C., Williams, B., Fry, M., Newton, G. and Wright, D. (2011), Three decades of water quality measurements from the Upper Severn experimental catchments at Plynlimon, Wales: an openly accessible data resource for research, modelling, environmental management and education, *Hydrol. Processes*, 25: 3818-30.

[18] Neal, C., Reynolds, B., Rowland, P., Norris, D., Kirchner, J.W., Neal, M., Sleep, D., Lawlor, A., Woods, C., Thacker, S., Guyatt, H., Vincent, C., Hockenhull, K., Wickham, H., Harman, S., Armstrong, L. (2012), High-frequency water quality time series in precipitation and streamflow: From fragmentsry signals to scientific challenge, *Science of the Total Environment*, doi: 10.1016/j.scitotenv.2011.10.072.

[19] Niemi, A.J. (1977), Residence time distribution of variable flow processes, *Int. J. Appl. Radiat. Isotopes*, 28: 855-860.

[20] Page, T., Beven, K.J., Freer, J. and Neal, C. (2007), Modelling the chloride signal at Plynlimon, Wales, using a modified dynamic TOPMODEL incorporating conservative chemical mixing (with uncertainty), *Hydrol. Processes*, 21: 292-307.

[21] Rinaldo, A., Botter, G., Bertuzzo, E., Uccelli, A., Settin, T. and Marani, M. (2006a), Transport at basin scales: Part 1. Theoretical framework, *Hydrol. Earth Syst. Sci.*, 10: 19-30.

[22] Rinaldo, A., Botter, G., Bertuzzo, E., Uccelli, A., Settin, T. and Marani, M. (2006b), Transport at basin scales: Part 2. Applications, *Hydrol. Earth Syst. Sci.*, 10: 31-48.

[23] Rinaldo, A., Beven, K.J., Bertuzzo, E., Nicotina, L., Davies, J., Fiori, A., Russo, D. and Botter, G. (2011), Catchment travel time distributions and water flow in soils, *Water Resour. Res.*, 47, W07537, doi: 10.1029/2011WR010478.

[24] Shand, P., Haria, A.H., Neal, C., Griffiths, K.J., Gooddy, D.C., Dixon, A.J., Hill, T., Buckley, D.K. and Cunningham, J.E. (2005), Hydrochemical heterogeneity in an upland catchment: further characterisation of the spatial, temporal and depth variations in soils, streams and groundwaters of the Plynlimon forested catchment, Wales, *Hydrology and Earth System Sciences*, 9: 621-634.

[25] Taiz, L. and E. Zeiger, (2010), Plant Physiology, Sinauer Assoc.